



**THE UNIVERSITY OF QUEENSLAND**

## **Bachelor of Engineering Thesis**

Influence of Carbides on the Impact Toughness  
and Wear Resistance of High Chromium Cast  
Irons

Student Name: Anson Nikhil Quadros

Course Code: MECH4501

Supervisor: Professor Mingxing Zhang

Submission Date: 30 May 2019

A thesis submitted in partial fulfillment of the requirements of the Bachelor of Engineering degree program in Materials Engineering

**School of Engineering**

**Faculty of Engineering, Architecture and Information Technology**

## **Acknowledgements**

I would firstly like to thank Prof. Mingxing Zhang for allowing me the opportunity to undertake this thesis project. Ming's guidance and mentoring has immensely helped me to complete this thesis.

I also would like to thank Mr. Jeffery Chang for his assistance and mentoring. Jeff's help and expertise in the field was crucial to my understanding of the subject matter. I would also like to thank Jeff for preparing the castings and getting the samples ready for us that were used in our experimental procedures.

## Abstract

The main aim of this project is to analyze the changes on how processes of heat treatment and strong carbide forming element additions would bring about changes in microstructure and mechanical properties of the eutectic A05 high chromium white cast iron. This included development of a suitable casting procedure to develop the alloys of different compositions.

Literature reviews have shown us that the strong carbide forming elements have a positive impact on HCCI's. Alloyed elements along with heat treatment process have shown major improvement in properties. Addition of Silicon along with heat treatment showed the transformation of the austenite matrix to martensite and greater the Si content, the denser were the secondary carbides in the matrix. This improved hardness and wear properties. Titanium & Niobium showed similar changes in properties. In fact, Niobium grain sizes had changed with increasing content improving the toughness. Research on destabilization treatment along with tempering showed large martensitic island forming which increased hardness. It is important to find the optimum destabilization time which is dependent on the C/Cr content (Figure 14). Tempering has been used to remove excess hardness upon heating. This helps in the formation of retained austenite to improve toughness.

To calculate the hardness values, Rockwell testing as well Vickers testing was conducted. Five different points were measured on the sample and the average value was taken and plotted as shown in Figure 30-33, 36 & 37. Three samples were used for the Charpy testing and the average of the three was taken as the Impact toughness value. Microstructural analysis was conducted using an optical microscope.

Destabilization treatment was conducted at  $950^{\circ}C$ ,  $1020^{\circ}C$ ,  $1080^{\circ}C$ ,  $1130^{\circ}C$ ,  $1190^{\circ}C$  for 6h. The impact toughness was seen to increase with increase in energy. Retained austenite was the main reason for this increase in toughness. Due to the martensitic transformation, energy dissipation takes place. The amount of energy dissipated determines the amount of retained austenite. As the tempering temperature increased the toughness reduced due to the decomposition of retained austenite. Hardness was seen to drop with increasing temperature but this was still higher than the as-cast state, hence showing improvement in wear and hardness properties.

Addition of Niobium saw a slight improvement in the hardness. At lower compositions the dispersed NbC carbides were more rod-like shaped. But at around 1-2% Nb, few of the particles changed their shape being more hexagonal giving its slight improvement in properties. Titanium addition saw a gradual increase in hardness up to about 1% Ti. Beyond this, the hardness just dropped. Very small particles were observed in the austenite matrix rather than in the carbides. A. Bedolla-Jaucinde found similar particles and on further examination using SEM and EDS, these were found to be Ti-rich particles. Hence, this could be a possibility.

The microstructural images did not show very clear and detailed changes in the microstructure even after these additions. This could be due to the fact that the casting temperature might not be high enough. Each alloy is different from each other and so the carbon/chromium content can determine formation of these carbides. Recommendations on how to possibly collect more accurate and distinctive results have been mentioned in the report.

# Table of Contents

1.0	Introduction.....	1
1.1	Aims .....	1
1.2	Scope .....	2
2.0	Literature Review.....	4
2.1	Chromium White Cast Irons.....	4
2.1.1	Microstructure of Hypoeutectic High Chromium White Cast Irons .....	4
2.1.2	Matrix Morphology .....	5
2.1.3	Carbide Morphology .....	6
2.2	Types of White Cast Irons.....	6
2.2.1	Hypoeutectic Cast Iron.....	6
2.2.2	Eutectic Cast Iron .....	7
2.2.3	Hypereutectic Cast iron.....	7
2.3	Strong Carbide Forming Elements .....	8
2.3.1	Silicon .....	8
2.3.1.1	Effect of Si on Microstructure and Wear Resistance of HCCI.....	8
2.3.2	Titanium.....	10
2.3.2.1	Effect of Titanium on the as-cast Microstructure of HCCI .....	10
2.3.2.2	Effect of Ti on the Properties of HCCI.....	12
2.3.3	Niobium.....	13
2.3.3.1	Effect of Niobium Addition on the Microstructure and Properties of HCCI .....	13
2.3.3.2	Microstructure and Wear resistance of Heat Treated HCCI Containing Nb .....	16
2.4	Heat Treatment Process.....	17
2.4.1	Destabilization.....	17
2.4.2	Tempering .....	18
2.4.3	Previous Investigations .....	18
2.5	Effect of Carbon Content on Microstructural Characteristics .....	20
2.6	Abrasive Wear .....	21
2.7	Critical Research Summary .....	23
3.0	Methodology.....	24
3.1	Sand Casting.....	24
3.2	Destabilization & Tempering Treatment.....	26
3.3	Cutting, Mounting, Polishing .....	27
3.4	Testing Equipment.....	28
3.5	Weight % Calculation.....	29
4.0	Results.....	30

4.1	Heat Treatment Results .....	30
4.1.1	Impact Toughness .....	30
4.1.2	Vickers & Rockwell Hardness .....	31
4.1.3	Microstructure .....	33
4.2	Titanium Addition Results.....	35
4.2.1	Vickers & Rockwell Hardness .....	35
4.3	Niobium Addition Results .....	36
4.3.1	Vickers & Rockwell Hardness .....	36
5.0	Discussion.....	38
5.1	Heat Treatment – Impact Toughness.....	38
5.2	Heat Treatment – Hardness .....	38
5.3	Niobium Addition.....	39
5.4	Titanium Addition .....	41
6.0	Conclusions.....	44
7.0	Recommendations.....	45
8.0	References.....	46
9.0	Appendices.....	48
	Appendix A – Titanium Addition Microstructure Images.....	48
	Appendix B - Niobium Addition Microstructure Images.....	49
	Appendix C – Destabilization Treatment Images.....	51
	Appendix D – Tempering Treatment Images .....	53
	Appendix E – Experimental Equipment Images.....	55

## List of Tables and Figures

Table 1: Vickers Hardness values for each of the iron phases in white cast iron.....	5
Table 2: Vickers Hardness values for different carbide types.....	6
Table 3: Chemical composition of the high chromium white cast iron.....	8
Table 4: Chemical composition of tested alloys (mass %)......	13
Table 5: Weight of Titanium required.....	29
Figure 1: Microstructure of as cast material.....	4
Figure 2: Micrograph of Hypoeutectic cast iron with C content of 2.7%.....	7
Figure 3: As-cast microstructure of the alloys.....	9
Figure 4: Microstructure after destabilizing treatment.....	10
Figure 5: SEM images at location 1mm below the surface.....	11
Figure 6: Effect of Ti conc. on volume fraction and diameter of carbides.....	12
Figure 7: Bending strength of the cylinders with diameter $\varnothing 20$ & $\varnothing 15$ mm.....	12
Figure 8: Rockwell Hardness values for the HCCI and Ti-added.....	13
Figure 9: SEM images with Nb addition.....	14
Figure 10: Mechanical properties changes with Nb addition.....	15
Figure 11: Heat treated samples at different Nb concentrations.....	16
Figure 12: SEM images of HCCI.....	16
Figure 13: Fracture Morphologies of specimens.....	17
Figure 14: Optimum destabilization treatment relative to chromium content.....	18
Figure 15: Microstructure after heat treatment at $970^{\circ}C$ for 2.5h.....	19
Figure 16: SEM images of Fe-Cr-C claddings.....	21
Figure 17: Abrasive wear mechanisms.....	22
Figure 18: Mass loss of pins under different loads.....	22
Figure 19: Sand mixer & coolest resin.....	24
Figure 20: Sand mould design.....	25
Figure 21: Sand levelled using flat head hammer.....	25
Figure 22: Complete sand mould set.....	26
Figure 23: Three samples placed for each temperature.....	26
Figure 24: Cutting machine and mounted samples images.....	27
Figure 25: Polishing machine and mats.....	28
Figure 26: Vickers Hardness & Optical Microscopy.....	28
Figure 27: Rockwell & Charpy Test equipment.....	29
Figure 28: Variation of Impact Energy with destabilization temperature.....	30
Figure 29: Variation of Impact Energy with tempering temperature.....	31
Figure 30: Variation of Vickers Hardness with destabilization temperature.....	31
Figure 31: Variation of Vickers Hardness with tempering temperature.....	32
Figure 32: Variation of Rockwell Hardness with destabilization temperature.....	32
Figure 33: Variation of Rockwell Hardness with tempering temperature.....	33

Figure 34: Heat treatment microstructure.....	34
Figure 35: Tempered specimen at 600 <sup>0</sup> C.....	35
Figure 36: Titanium addition.....	36
Figure 37: Niobium addition.....	37
Figure 38: A05 alloy with 0 wt. % Nb.....	40
Figure 39: A05 alloy with 0.5 wt. % Nb.....	40
Figure 40: A05 alloy with 2 wt. % Nb.....	41
Figure 41: A05 alloy with 0 wt. % Ti.....	42
Figure 42: A05 alloy with 1 wt. % Ti.....	42
Figure 43: A05 alloy with 2 wt. % Ti.....	43
Figure 44: A05 alloy with 0.5 wt. % Ti.....	48
Figure 45: A05 alloy with 1.0 wt. % Ti.....	48
Figure 46: A05 alloy with 2 wt. % Ti.....	49
Figure 47: A05 alloy with 0.5 wt. % Nb.....	49
Figure 48: A05 alloy with 1 wt. % Nb.....	50
Figure 49: A05 alloy with 2 wt. % Nb.....	50
Figure 50: A05 alloy heat treated at 950 <sup>0</sup> C for 6h.....	51
Figure 51: A05 alloy heat treated at 1020 <sup>0</sup> C for 6h.....	51
Figure 52: A05 alloy heat treated at 1080 <sup>0</sup> C for 6h.....	52
Figure 53: A05 alloy heat treated at 1190 <sup>0</sup> C for 6h.....	52
Figure 54: A05 alloy tempered at 260 <sup>0</sup> C for 3h.....	53
Figure 55: A05 alloy tempered at 320 <sup>0</sup> C for 3h.....	53
Figure 56: A05 alloy tempered at 600 <sup>0</sup> C for 3h.....	54
Figure 57: A05 alloy in the as-cast state.....	54
Figure 58: Furnace used for destabilization and tempering treatment.....	55
Figure 59: Polyfast resin used for sample mounting.....	55
Figure 60: Coke used to prevent oxidation during heat treatment.....	56



## 1.0 Introduction

High Chromium White Cast Irons (HCCI) are erosion resistant ferrous alloys that are widely used in manufacturing [1]. They are generally known for their excellent abrasion and wear resistance properties. Due to this feature, they are widely used in a number of applications such as cement manufacturing industries, slurry pumps, grinding balls, earth handling and materials/mineral industries. The reason for this excellent property is due to the impartment of hard eutectic carbides that are present in the microstructure. Furthermore, role of the matrix, including austenite and martensite or a mixture of the two, prevent sufficient mechanical support to prevent the carbide from cracking and spalling [2].

For this project, a eutectic HCCI alloy, primarily known as A05 was used for various experimental procedures. This alloy had a Carbon content of 2.85 wt% and Chromium content of 26.57 wt%. With this range of chromium content used, the main carbide formed is the  $M_7C_3$ . This carbide is hard and brittle, resulting in easy path for crack propagation. This therefore limits its application in environments that involve high impacts, and hence the toughness is reduced.

Over the years, various researchers have proposed a number of ways to try and tackle this problem. In order to improve the property of toughness of white cast iron, it was suggested to try and alter the matrix as they play an important role in determining fracture toughness. Others have focused on the morphology and characteristics of secondary carbides during heat treatments. Different parameters of heat treatment and different compositional characteristics, play a vital role in the morphology and orientation of microstructure. The addition of alloying elements such as Ti, Nb or V have also been studied and are able to refine microstructures of the HCCIs to some extent. This research project will investigate the potential for enhancement of wear resistance and toughness through methods of heat treatment and addition of strong carbide forming (SCF) alloying elements.

### 1.1 Aims

The primary aims of the project are as follows:

1. To be able to effectively compare the changes in properties observed through different parameters and conditions of heat treatment and addition of SCF elements.
2. To verify the expectation that heat treatment and addition of SCF will enhance toughness, hardness & wear resistance of A05 alloy.
3. Identifying potential explanations for any observed differences in toughness, hardness & wear performance.
4. To be able to explain as to why each of these added SCF elements show improvement/ no improvement in properties.

The secondary aims of the project are as follows:

1. Exploring the morphology and compositions of different carbides formed by each SCF element.
2. To be able to assess and explain the accuracy of the different methods used in this experimental process.

## **1.2 Scope**

This project is an industrially funded research and development venture conducted through the cooperative efforts of UQ and The Weir Group at the University of Queensland. As mentioned, the investigation is on the influence of carbides on the impact toughness and wear resistance of high chromium cast irons. The findings have been considered as an 'initial step' for this project, and will provide motivation for further extensive research in the future.

The HCCI selected for this series of experiments is of the composition 26.57Cr- 2.85C- 1.97Mn- 0.44Si- 0.42Ni- 0.12Cu- 0.029S- 0.023P. This composition was selected as it is a Eutectic HCCI alloy (A05) and its property changes and effects were compared with results from a Hypereutectic HCCI alloy (A61) undergoing same testing procedures (work on this alloy was done by another student.). It would be beneficial to verify the wear and toughness enhancement for a range of HCCI alloys, however this falls beyond our scope.

The chosen SCF elements that were investigated were Titanium (Ti) and Niobium (Nb). The carbide characteristics of Chromium were also indirectly assessed due to their presence in the

baseline white cast irons. Other SCF elements like Molybdenum (Mo), Silicon (Si), and Tungsten (W) were not used for investigation due to the difficulties in acquiring these raw materials.

The overall project was mainly divided into two parts. The first being the investigation of property change on different heat treatment parameters and the second being the investigation with respect addition of Nb and Ti at various compositions through sand casting process.

For the first part, with the heat treatment process, five different temperatures were selected ( $950^{\circ}\text{C}$ ,  $1020^{\circ}\text{C}$ ,  $1080^{\circ}\text{C}$ ,  $1130^{\circ}\text{C}$ ,  $1190^{\circ}\text{C}$ ) and the A05 samples were heated for 6 hours in the furnaces available in the heat treatment labs. This was then followed by tempering at four different temperatures of ( $260^{\circ}\text{C}$ ,  $320^{\circ}\text{C}$ ,  $500^{\circ}\text{C}$ ,  $600^{\circ}\text{C}$ ) for 3 hours. Standard Operating Procedures were followed to enable the safe, smooth and accurate conduct of this experiment.

The second part includes the addition of Ti and Nb through sand casting process. Compositions of 0%, 0.5%, 1%, 2% were used for each of these elements to be added. Adapted casting methods and steps were followed to enable the safe production of the melted alloy and then being poured into the mold.

To determine the hardness of these samples, Vickers and Rockwell hardness test equipment's were used. The Vickers testing method determines the hardness of certain microstructural constituents whereas the Rockwell determines hardness for the overall gross microstructure. Next, toughness results were obtained by using the Charpy test equipment. It determines the energy (in Joules) required to break the sample. The samples were cut to size, mounted, polished and etched before the above mentioned tests were conducted. Optical microscope was used to verify the presence of SCF carbides and provide potential explanation on these microstructures. The use of scanning electron microscopy (SEM) and Energy Dispersive X-ray Spectroscopy (EDS) was considered out of scope for the purpose of this project.

## 2.0 Literature Review

### 2.1 Chromium White Cast Irons

As the name suggests, white cast iron is essentially an alloy with more than 1.7% carbon and a few other varying but limited amounts of silicon, manganese, Sulphur and phosphorus [3]. Special elements such as nickel, chromium etc. are added to try and improve the physical and mechanical properties. Most of the parts used in machining are made of white cast irons. In general, heat treatment is done on these parts to improve machinability and obtain the optimal microstructure.

#### 2.1.1 Microstructure of Hypoeutectic High Chromium White Cast Irons

The content of chromium has a very important role to play in the formation of carbides. It is found that at about 10 wt. % Cr, formation of eutectic  $M_3C$  takes place. With increase in the chromium content the properties have also seen to improve due to the formation of more carbides in the microstructure. In our case, with 26.57 wt. % Cr the microstructure contains  $M_7C_3$  carbides. These chromium rich carbides are surrounded by an alloyed steel matrix. Figure 1 below represents the microstructure of a as cast hypoeutectic HCCI.

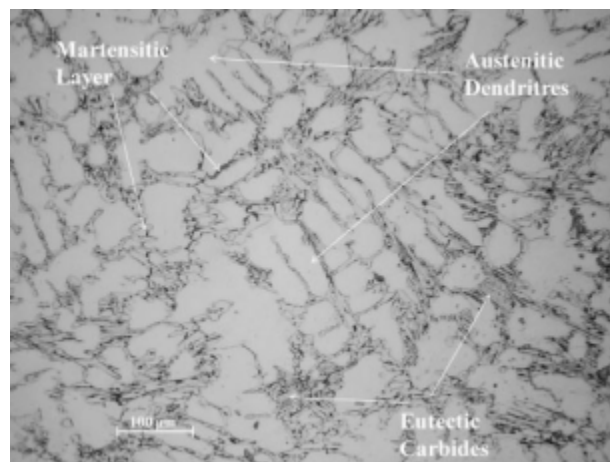


Figure 1: Microstructure of as cast material [4]

As seen from the figure above, it is observed that the solidification process starts with the nucleation of primary austenitic dendrites. This is then followed up with a eutectic mixture of the austenite (primarily known as the  $\gamma$  phase) with the eutectic  $M_7C_3$  carbides [5]. At ambient temperatures the HCCI have an austenitic matrix within which the chromium carbides have been

dispersed. On close observation we also notice the existence of dark martensitic layers surrounding the eutectic carbides. Therefore, the properties of these materials are influenced by the morphology, size and distribution of these phases in the microstructure.

### 2.1.2 Matrix Morphology

One of the main flexibilities exhibited is the possibility of HCCI's to have different matrix structures in different stages of treatment. Some of which are austenite, pearlite, martensite or a combination of these. The hardness values for these white cast irons with these matrices are listed in Table 1.

**Table 1: Vickers Hardness values for each of the iron phases in white cast iron [6]**

<b>Matrix</b>	<b>Vickers Hardness (HV)</b>
Pearlite	250-460
Austenite	300-600
Martensite	500-1010

The general observation over the years say that harder the material, higher is the wear resistance. It is also understood that the formation of ferrite or pearlite in these white cast irons does dramatically reduce the abrasion resistance of materials due to the poor support of carbides [2]. Ideally to obtain the hardest material, we would require all of the austenite to completely transfer to martensite due to its hardness values. But in reality this is difficult to achieve due to large levels of retained austenite in the as cast state. The austenite transforms to martensite through stress induced mechanism which provide good support to the carbides. However, researchers believe that the presence of retained austenite in the matrix results in the best abrasion resistance [2]. Though there is a high percentage of Cr content, the majority is engaged in the carbides, leaving the matrix Cr deficient. Addition of alloying elements like Mo, Ni, Cu etc. have found to increase hardenability [4].

With regards to toughness, it was found that the matrix plays a critical role in determining fracture toughness through its ability to stop crack propagation. The toughness of the austenite matrix is found to be higher than the martensitic matrix, and as the volume fraction of austenite increases,

so does the fracture toughness [2]. Therefore, for optimum abrasion resistance and toughness a martensitic matrix is desired with good percentage of retained austenite present.

### 2.1.3 Carbide Morphology

With the range of chromium content used, the main carbide formed in this case is the  $M_7C_3$  carbide. On heat treatment, extensive precipitation of secondary carbides take place but are smaller in size when compared to the  $M_7C_3$ . The type, size, morphology of the eutectic carbide play a huge role in influencing the properties of the iron [6]. As mentioned in Section 2.1.1, in a hypoeutectic structure we have two main carbides i.e.  $M_7C_3$  and  $M_3C$ . The  $M_{23}C_6$  is rarely seen in commercial irons and is only found when there is a high percentage of chromium irons involved. The hardness values for these carbide types have been listed in Table 2.

**Table 2: Vickers Hardness values for different carbide types [7]**

Carbide Type	Vickers Hardness (HV)
$M_3C$	800-1100
$M_7C_3$	1000-1800
$M_{23}C_6$	~1000

Carbide is a strong forming element and the  $M_7C_3$  carbide produces the maximum hardness. It is also said to have a rod shaped morphology compared to the  $M_3C$  which has a plate like morphology. The stable  $M_7C_3$  is formed at chromium concentrations ranging from 12% - 26%. This eutectic carbide is desirable as it is best able to resist abrasion from particles due to its high hardness.

## 2.2 Types of White Cast Irons

Depending on the carbon content, white cast irons can be divided into three main classes: hypoeutectic, eutectic and hypereutectic cast iron. Each of these three classes have different microstructure formation, solidification and cooling rates.

### 2.2.1 Hypoeutectic Cast Iron

Here, only the austenite primary crystals are precipitated from the melt when the liquidus line is reached. This increases the carbon content in the residual melt. The melt crystallizes to form a eutectic mixture of the austenite and cementite. As cooling progresses, due to the decrease in

solubility of carbon, cementite is precipitated as the primary austenite and austenite crystals are contained in the eutectic mixture [8]. At lower carbon content of about ~2.7%, dark pearlite spots are observed as show below in Figure 2. This pearlite microstructure consists of ferrite and lamellar cementite. With increasing carbon content, there are significantly larger proportions of eutectic matrix compared to pearlite.

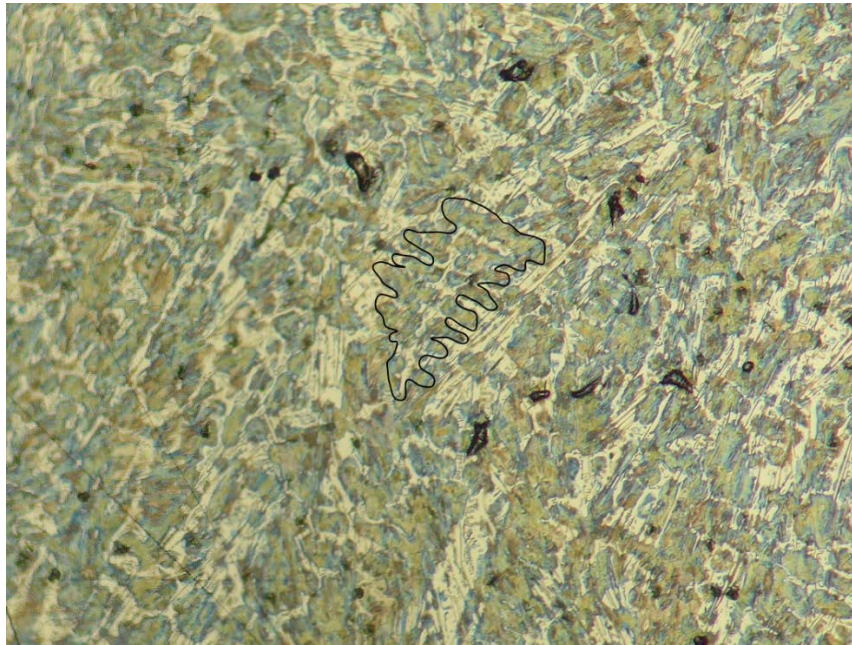


**Figure 2: Micrograph of Hypoeutectic cast iron with C content of 2.7% [8]**

### **2.2.2 Eutectic Cast Iron**

If the cast iron has the eutectic composition of 4.3% carbon, then on cooling from the liquid phase, at the eutectic temperature, the liquid phase solidifies to two solid phases. Due to this, a fine mixture of austenite and cementite is formed. As solidification progresses, the austenite crystals present in this fine mixture are completely saturated and show maximum possible concentration of carbon that is soluble in the austenite. As further cooling takes place, the solubility decreases and the austenite crystals permanently precipitate cementite [8].

### **2.2.3 Hypereutectic Cast iron**

In this case, only primary cementite with needle like structure crystallizes during solidification. After solidification, this cementite structure is embedded in the surrounding eutectic mixture of austenite and cementite. As temperature is lowered, the austenite in the eutectic undergoes

cementite precipitation when temperature is lowered. Thus, at even more cooling, the carbon content drops and so it converts to pearlite.

## **2.3 Strong Carbide Forming Elements**

Strong Carbide forming elements are those which have a high affinity for carbon and readily form carbides. These elements help in improving the properties of cast iron through their effect on the matrix [9]. Some of the commonly used alloying elements are manganese, copper, nickel, niobium, titanium and silicon. According to researchers, these elements did bring about a positive impact to the HCCI properties and microstructure. The impacts of some of these elements on HCCI have been critically reviewed and presented below in the following sections.

### **2.3.1 Silicon**

#### **2.3.1.1 Effect of Si on Microstructure and Wear Resistance of HCCI**

Si addition from 0.5 to 1.5 wt. % were studied. These alloys were melted in the induction furnace and cast into a cylindrical metal mould [10]. The chemical composition of the HCCI has been provided in Table 3.

**Table 3. Chemical composition of the high chromium white cast iron (wt.%). [10]**

<b>Alloy</b>	<b>C</b>	<b>Si</b>	<b>Mn</b>	<b>Cr</b>	<b>Mo</b>
A	2.81	0.50	0.61	18.1	0.85
B	2.82	1.50	0.62	18.2	0.83

All specimens were destabilized at 950°C for 3 h, followed by quenching in the air at room temperature and then tempered at 200°C for 6 h to get a tempered martensitic matrix and released stress.

As shown in Figure 3 below, we observe the as cast microstructures images for alloy A and B. For alloy A the carbides are of hexagonal shape and exhibited different structures with different orientations. For alloy B, the microstructure had finer eutectic carbides as compared to alloy A [10]. On observation using an SEM, austenitic matrix was observed in alloy A and pearlitic matrix in the alloy B. The reason for this transformation from austenitic matrix to pearlite is because as



the Si content increases, the solubility of carbon in the matrix increases and lowers stability of austenite at high temperature.

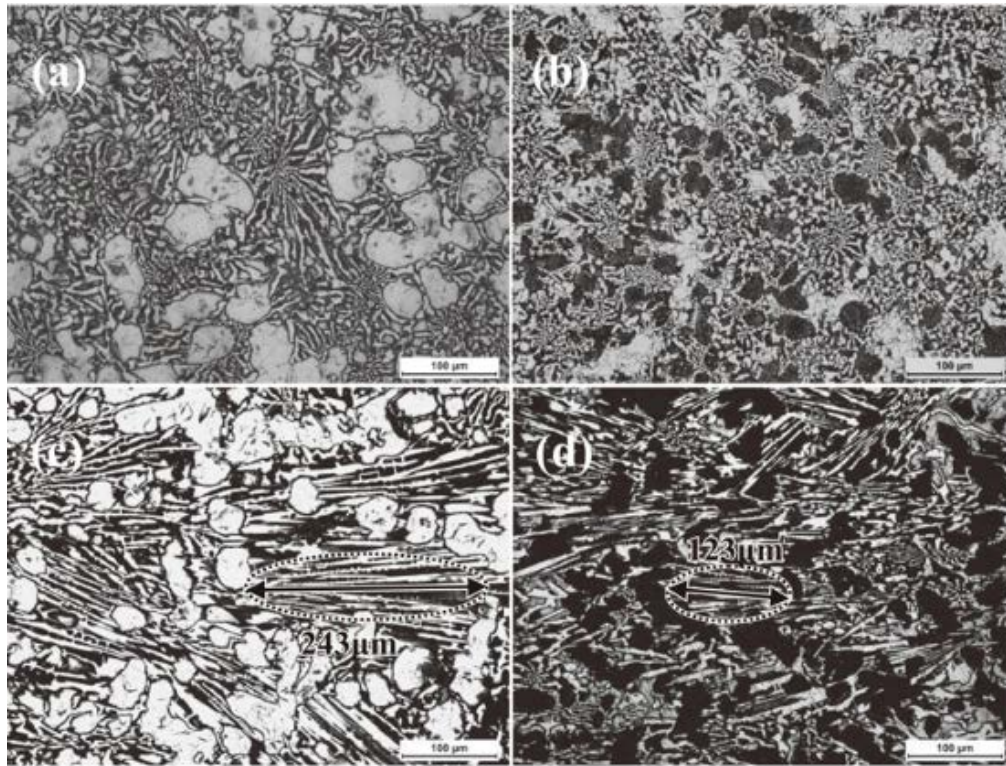


**Figure 3: As-cast microstructure of the alloys: (a,c) alloy A at positions A and B, respectively; (b,d) alloy B at position A and B, respectively. [10]**

It is a well-known fact that in order to achieve improved wear properties destabilization treatment is preferred where the austenite matrix would transform to martensitic matrix. From Figure 4 below, we see that with increase in Si content, the precipitation of secondary carbides increases. On further magnification alloy B has denser secondary carbides precipitated. This resulted in an improvement in the microhardness of the matrix and macrohardness of the surface. Abrasive wear tests also proved that alloy B had lesser mass loss at higher loads compared to A due to the denser secondary carbides.

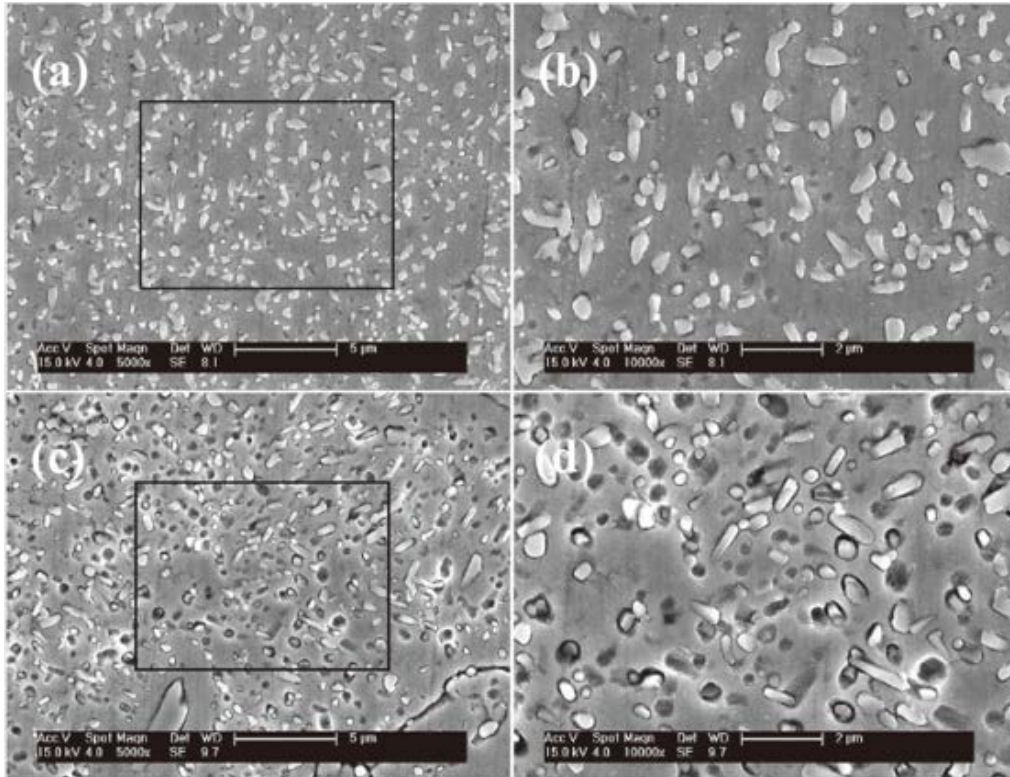


**Figure 4: Microstructures after destabilizing treatment: (a,b (magnified)) alloy A; (c,d (magnified)) alloy B [10].**

## 2.3.2 Titanium

### 2.3.2.1 Effect of Titanium on the as-cast Microstructure of HCCI

Titanium was added to the as-cast microstructure of hypereutectic high-Cr cast iron containing 4.0 wt. % carbon and 20 wt. % chromium [11]. The hypereutectic alloys are known to have a large volume fraction of the hard and wear resistant  $M_7C_3$  carbides which makes it the preferred choice for hardfacing applications. However, hypereutectic HCCIs generally are not favored for casting, due to high rejection rates caused by the large primary carbides present [11]. The aim is to try and improve its castability by adding different amounts of titanium.

Compositions of 0, 0.51, 0.95 and 1.47 wt. % Ti were added to the HCCI. Figure 5, below displays the microstructure observed using an SEM for compositions of 0.51, 0.95 and 1.47 wt. %. The following observations were noted.

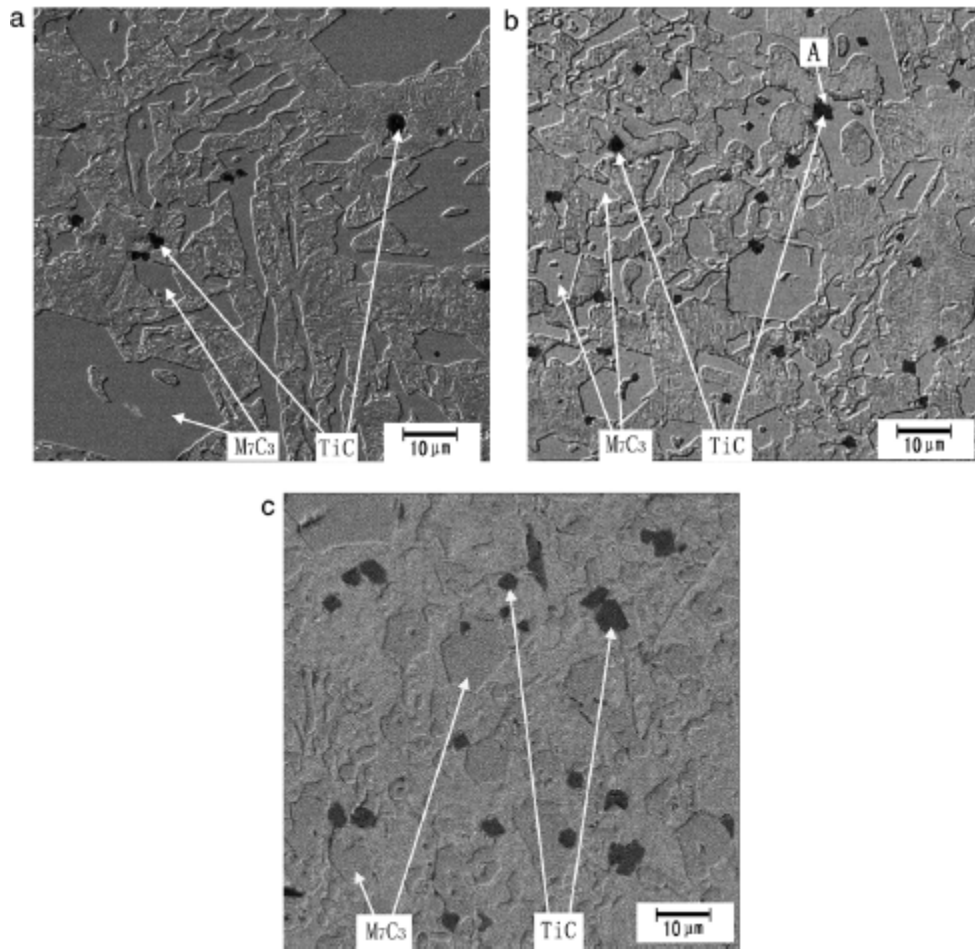


**Figure 5: SEM images at location 1mm below the surface, a) specimen 2; b) specimen 3; c) specimen 4 [11]**

From these images above, it was confirmed that the black particles observed were indeed TiC particles. We observe a refinement in the primary carbides with an increase of titanium concentration. These black TiC particles are seen to be dispersed in and around the carbides. With this increase in concentration to about 1.47 wt. %, the diameter of these particles have started to grow larger and agglomerated [11]. Therefore it can be inferred that it is not right to increase the concentration unlimitedly.

Furthermore, Figure 6 displays a plot between Ti content vs. carbide volume fraction. With the increasing size of the TiC particles, the average diameter and the carbide volume fraction decreases with increasing concentration. This is due to the fact that the TiC particles precipitate first prior to the  $M_7C_3$  carbides and this consumes part of these carbides, decreasing their volume fraction.

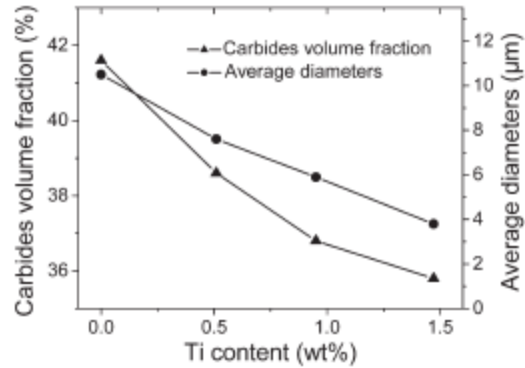


**Figure 6: Effect of Ti conc. On volume fraction and diameter of carbides [11].**

When solving equations for Ti solubility in HCCI, it was observed that the Ti solubility in the melt is only about 0.03%. Since we are dealing with higher values of Ti concentration being added to the melt at the precipitation temperature, TiC particles form first before the primary carbides. The fact that there is also a decrease in carbide volume fraction with increasing concentration, is also in agreement with the fact that the TiC particles precipitate first.

### **2.3.2.2 Effect of Ti on the Properties of HCCI**

Ti-addition also have a significant impact not just on the microstructure, but also on the mechanical properties of HCCI. Here, two sets of cylinders with different dimensions were casted ( $\phi 20$  mm,  $\phi 15$  mm x 250 mm). Titanium added in this case was about 4% by mass. The mechanical properties tested in this case where the bending strength and the Rockwell hardness. Figure 7 show the bending strength of the two samples after the test was completed [12].

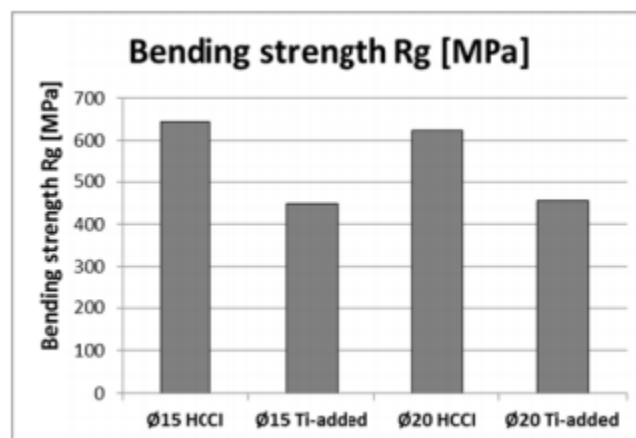


**Figure 7: Bending strength of the cylinders with diameter  $\phi 20$  mm &  $\phi 15$  mm [12]**

It is observed that the bending strength has decreased with the addition of Ti to both the samples. This is because of the refinement of the primary grains due to this high mass % addition of Ti. The

crystallization time also played an important role in bringing about this property change. The crystallization time decreased with the addition of Ti. As seen in Section 2.3.2.1, formation of TiC carbides take place that leads to saturation of carbon resulting in the formation of  $M_3C$  carbide type.

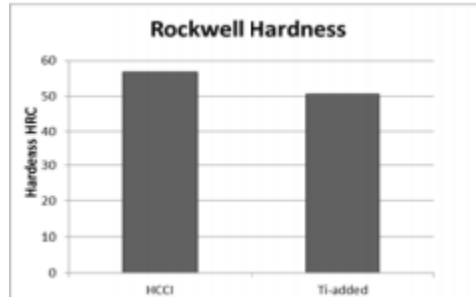


**Figure 8: Rockwell Hardness values for the HCCI and Ti-added [12].**

Figure 8, shows us the Rockwell Hardness test results. The addition of titanium shows a decrease in hardness value. As mentioned above, the  $M_3C$  carbide are formed which are known to have lower hardness compared to the  $M_7C_3$  carbides existing in the matrix [12]. A suggestion to try and improve these properties would be to control the structure by increasing the carbon content to obtain carbides of  $M_7C_3$  type.

### 2.3.3 Niobium

#### 2.3.3.1 Effect of Niobium Addition on the Microstructure and Properties of HCCI

Niobium of 0.5 mass % and 2 mass % were added to hypoeutectic white cast iron containing 19 mass % Cr and 2.9 mass % C [13]. The aim is to try and achieve a simultaneous improvement in toughness and wear resistant properties through the formation of carbide with greater hardness and reduces the carbon content of the matrix. From past research papers, NbC has been shown to improve the hardness properties. But, not much work has been done on fracture toughness improvement. There is still a question as to how much mass % of Nb should be added to the HCCI to obtain optimal fracture toughness. Table 4 below gives us the chemical composition of the tested alloys.

Alloy	C	Cr	Mn	Cu	Ni	Mo	Si	Nb
1	2.89	19.03	0.71	0.99	0.103	0.48	0.85	—
2	2.93	18.86	0.78	0.91	0.087	0.52	0.81	0.54
3	2.91	19.14	0.75	0.96	0.108	0.49	0.79	2.06

**Table 4: Chemical Composition of tested alloys (mass %) [13]**

With regards to microstructure, Figure 9 shows us SEM images of the two Nb compositions. At 0.54 % Nb, NbC are formed in the eutectic mixture of the  $M_7C_3$  carbides and austenite. These carbides are seen to have petal like shapes at this composition. With increase in concentration, the NbC are more compact and appear as nodular or hexagonal disc carbides [13]. There is not much change observed with the amount of retained austenite with the addition of Nb. With increase in the Nb content volume fraction of carbides decreases.

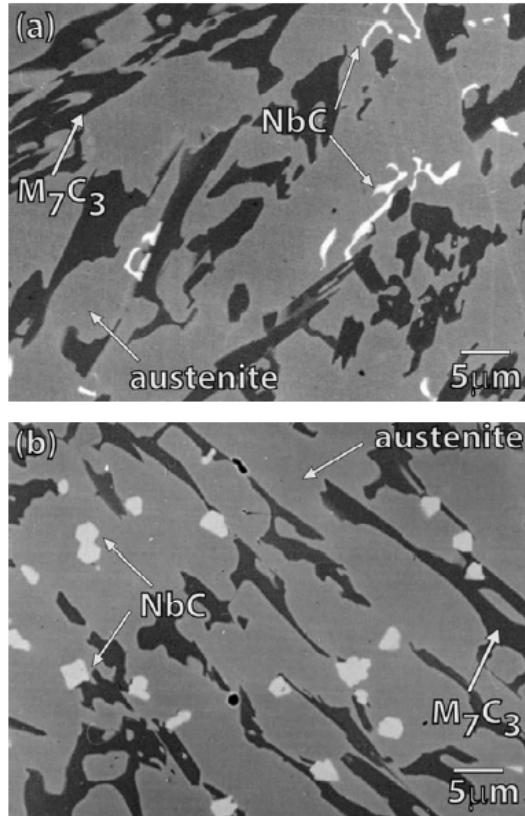
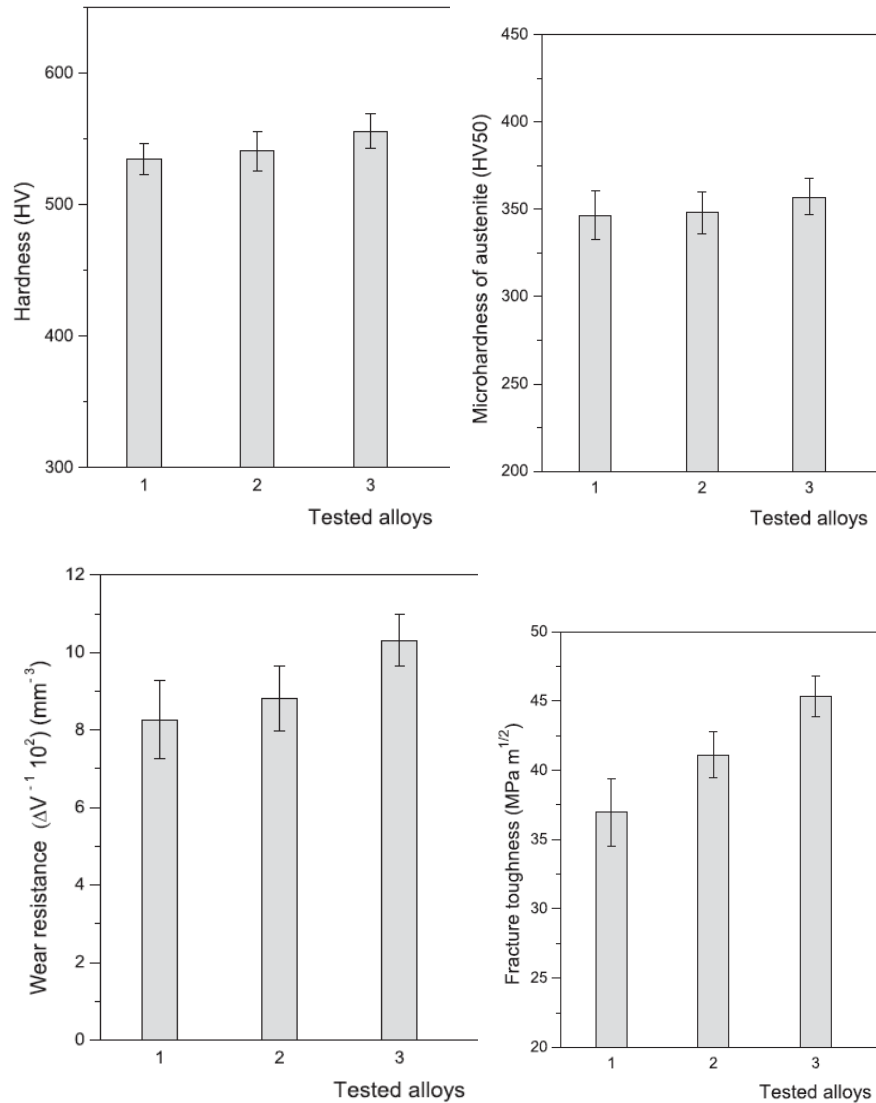


Figure 9: SEM images with Nb addition at (a) 0.54% Nb; (b) 2.06% Nb [13]

Considering the mechanical properties like hardness, microhardness, fracture toughness and wear resistance, it was observed that Niobium did have an influence in these properties. They were slight increase in hardness and microhardness observed with increase in Nb content. A much bigger increased was noticed with regards to fracture toughness and wear resistance. Figure 10 shows these results below.



**Figure 10: (a) Hardness; (b) Microhardness; (c) Wear Resistance; (d) Fracture Toughness [13]**

We observed from Figure 9 that microstructural changes did take place with Nb addition. The majority of niobium present in the alloy is of the MC carbide type because of the low solubility of Nb in the austenite [13]. At Nb composition of 0.54%, from research papers, we know that solidification starts with formation of  $\gamma$ -phase in this alloy. As solidification progresses, due to the low solubility of Nb, carbon and chromium, these accumulate in front of the solid-liquid interface [13]. As the temperature lowers, the eutectic reaction takes place, the eutectic composed of NbC and austenite was developed. These NbC particles further block the  $\gamma$ -phase growth. At Nb composition of 2.06% the NbC carbides can act as the substrates for heterogeneous nucleation of the austenite dendrites, which results in significant refinement of the final grain size.

### 2.3.3.2 Microstructure and Wear resistance of Heat Treated HCCI Containing Nb

We have observed how the properties and microstructure changes with the addition of Nb to HCCI. We now look at what happens when Nb is added to HCCI that have been heat treated. A hypereutectic HCCI was examined with  $>30$  wt. % Cr and  $>4$  wt. % C [14]. Varying Nb contents of 0, 0.48 and 0.74 (wt. %) were used. The heat treatment process by destabilization took place at  $1050^{\circ}\text{C}$  for 2h, followed by air cooling to room temperature. After which, tempering was carried out at  $250^{\circ}\text{C}$  for 2h [14]. Figure 11 below shows the heat treated samples with different Nb concentrations.

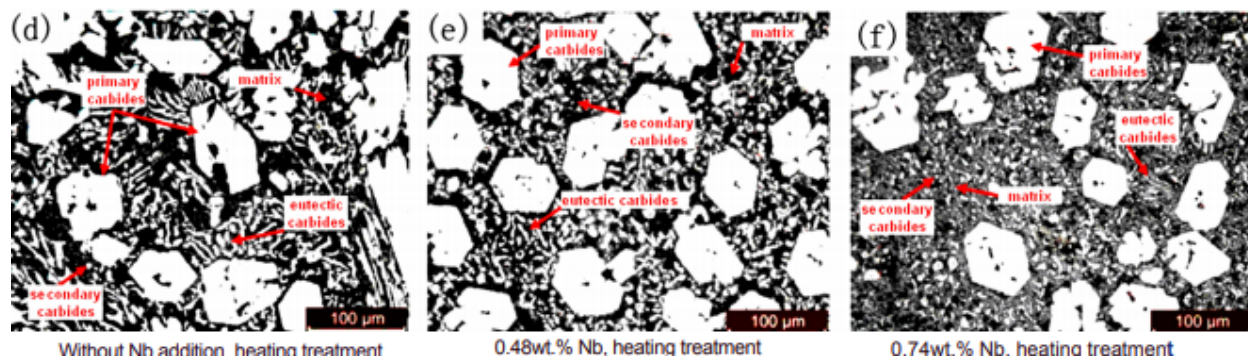


Figure 11: Heat Treated Samples at different Nb concentrations [14]

From these heat treated samples it is observed that the primary carbides have more a hexagonal shape and this doesn't change with increasing Nb content. Also, another interesting aspect is the increase in the amount of secondary carbides as Nb content increases. These carbides have come along due to the destabilization of the eutectic austenite [14]. Backscattered images from Figure 12, go on to show that the white NbC particles are present in and around the edges of the primary hexagonal carbides. The NbC particles increase with increase in Nb content how their size shows little variation. This observation is found to be consistent in many of the research papers [14].

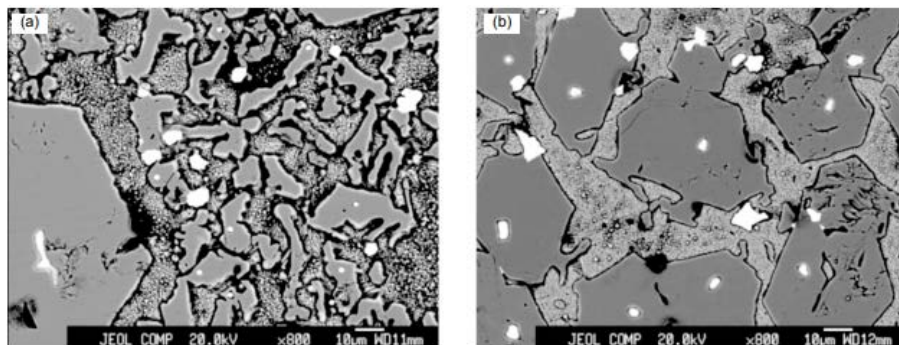
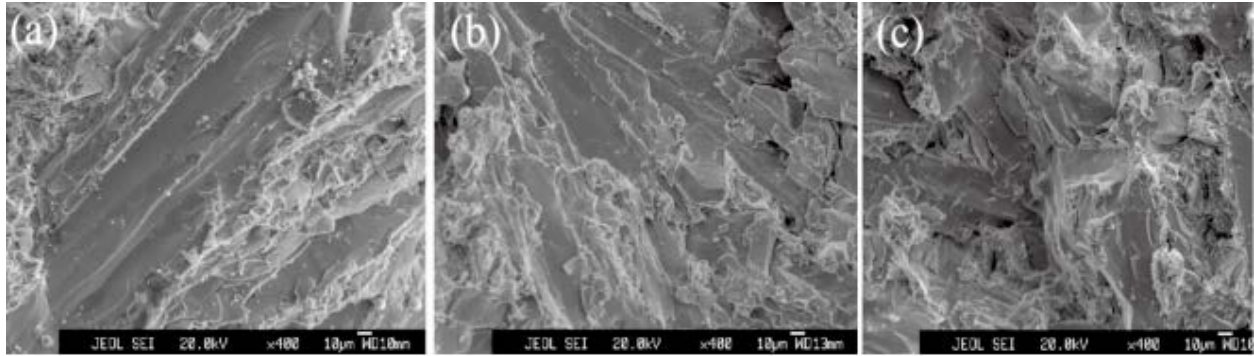


Figure 12: SEM images of HCCI containing (a) 0.48 wt. % Nb and (b) 0.74 wt. % Nb



From Section 2.3.3.1, we saw that the fracture toughness with increasing Nb content showed an improvement in the as cast state. This same trend was observed with the heat treated samples as well. However, from Figure 13 below, a key observation noted was the river patterns that could be found in specimen without Nb addition (Fig 13[a]). They were formed by the crack moving through the crystal along a number of parallel planes, which are indication of the absorption of energy by local deformation. This results in brittle fracture mechanism. With the addition of Nb these river patterns are less visible resulting in an increase in fracture toughness [14].



**Figure 13: Fracture Morphologies of specimens (a) 0 wt. % Nb, (b) 0.48 wt. % Nb, (c) 0.74 wt. % Nb [14]**

Considering the wear properties, the weight loss of the HCCI containing Nb decreased with increasing Nb content when heavier loads were used. This shows that the wear properties have actually improved with the addition of Nb at heavier loads [14].

## **2.4 Heat Treatment Process**

As previously mentioned before, HCCI are known for their good wear and abrasion resistance and they have been applied in a different kinds of environments. From past researchers, heat treatment has found to modify microstructure and improve properties. It is a well-known fact that the toughness is a property that is an area of improvement and so various conditions of heat treatment have shown an increase in toughness whilst maintaining the wear properties. Two critical heat treatments which may be applied are destabilization and tempering [15].

### **2.4.1 Destabilization**

From Section 2.1.2, martensite was found to have the highest range of hardness value. Therefore, in order to change the as-cast microstructure from austenite to martensite, destabilization treatment is performed. By doing so, refinement of the primary  $M_7C_3$  carbides take place reducing the carbon content in the matrix and improving abrasion resistance. During the air cooling process after being

heat treated, the austenite to martensite transformation takes place. The general heat treatment time would go on from anywhere between 2-6h or even longer. The optimum destabilization temperature is dependent on the alloy content, with higher chromium to carbon ratio requiring higher temperatures. These temperatures range between 930 and 1060°C, dependent on the chromium to carbon ratio (Cr/C) [7]. Figure 14 below shows the optimum destabilization temperature relative to chromium content.

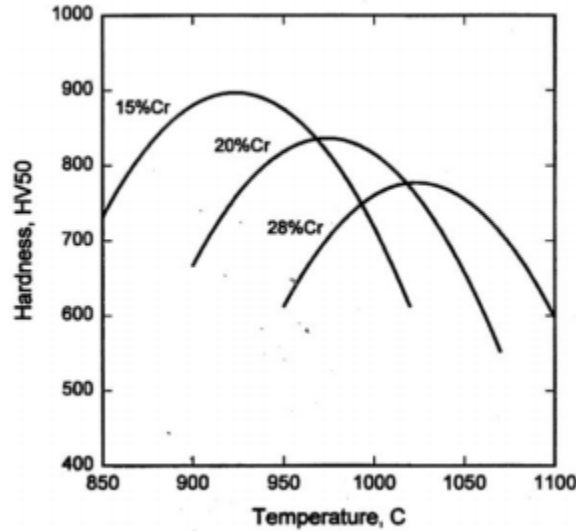


Figure 14: Optimum destabilization temperature relative to chromium content. [7]

### 2.4.2 Tempering

Once the destabilization process is complete followed by air cooling, the material is known to be quite hard. To remove this excess residual stresses present in the iron, tempering is done. This is a process of heat treating below a critical point for a certain period of time, followed by air cooling. This not only remove the excess hardness but also is used to increase the toughness of iron-based alloys. The exact tempering temperature depends on the composition of the alloys and desired properties [16].

### 2.4.3 Previous Investigations

E. Karantzalis, A. Lekatou & H. Mavros had worked on different conditions of critical subcritical heat treatments. They found each of these conditions brought about a different change in microstructure. One such condition was to heat the specimen with composition of 2.35% C, 18.23% Cr and 0.58% Mo to about 970°C for 2.5h. The microstructure had a drastic change when compared to Figure 1. The small martensitic layers observed in Figure 1 had grown into large dark

islands in the eutectic carbide/austenite matrix. On further observation using an SEM, extensive precipitation of secondary carbides were observed. These carbides had a cuboidal morphology. Figure 15 shows these martensitic islands.

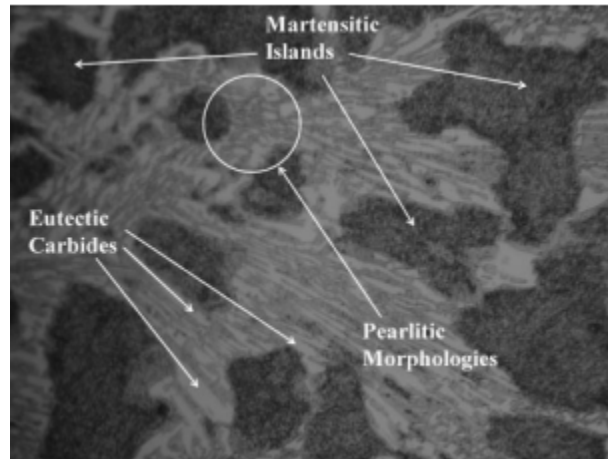


**Figure 15: Microstructure after heat treatment at 970<sup>0</sup>C for 2.5h [4]**

M. Zhang, P. Kelly & J. Gates had also studied heat treatment effects on the mechanical properties like toughness and hardness. Austenitization took place at 5 different temperature for 6h followed by air cooling. This was then followed by tempering at 200<sup>0</sup>C for 3 hours [2]. It was observed that as the destabilization temperature had increased, the impact toughness also increased. But with regards to tempering the highest toughness was obtained between 200 to 250<sup>0</sup>C after which the toughness just dropped. From this we could say that tempering brings about positive changes to the toughness only up to a certain limit after which it drops. This helps in identifying the optimum tempering temperature.

Vickers hardness testing on these samples were done. At temperatures as low as 950<sup>0</sup>C, there was a sharp rise in hardness compared to the as-cast state. But as the temperature increased, the hardness dropped considerably. On Tempering, the hardness slightly reduces from the untempered material but after the temperature is higher than 400<sup>0</sup>C the hardness just increases. This is attributed due to the secondary hardening [2].

H. Gasan and F. Erturk had also conducted similar tests to check property behaviors at 900<sup>0</sup>, 1000<sup>0</sup> and 1100<sup>0</sup> C for 2 hours. With regards to microstructure it was observed that with increase in temperature, the amount of secondary carbides became fewer in size and coarser [17]. The bulk hardness of the as cast state was found to be much lower than the hardness at the

destabilization temperatures. The hardness reaches a peak at 1000<sup>o</sup> C after which it drops down but, still higher than the as cast state. The reason for this drop in hardness is attributed due to the influence of carbide volume fraction and reduction in amount of martensite. The wear results also show that at different sliding speeds, the as cast material had a lot more wear compared to the heat treated samples. This again traces back to the fact that the increase in hardness has a huge role to play along with the precipitation of secondary carbides [17].

From all these investigations we see that heat treatment influences the HCCI properties quite a lot. Different combinations of temperatures and cooling time gives us different results. It is also to be noted that heating at the highest temperature will not always give the best properties. Finding the optimum temperature is key. This optimum temperature value can change with different compositions of carbon and chromium content. Alloy addition and their concentrations also play an important role in finding this ideal temperature.

## **2.5 Effect of Carbon Content on Microstructural Characteristics**

C. Chang et al. studied the relationship between the morphology of primary carbides and the carbon content of hypereutectic Fe-Cr-C claddings [18]. Claddings with three carbon contents of 3.73, 4.21 & 4.85 wt. % were deposited on the ASTM A36 base metal by arc welding [18]. It was observed that as the amount of carbon content increased, the fraction of proeutectic  $(Cr, Fe)_7C_3$  carbides increased. These proeutectic carbides had rod-like and blade-like shapes at low carbon contents. But, with increase in the carbon content, the proeutectic carbides size decreased from 59.00 to 13.53 $\mu m$  [18]. Figure 16 below represents the SEM images for each of these contents.

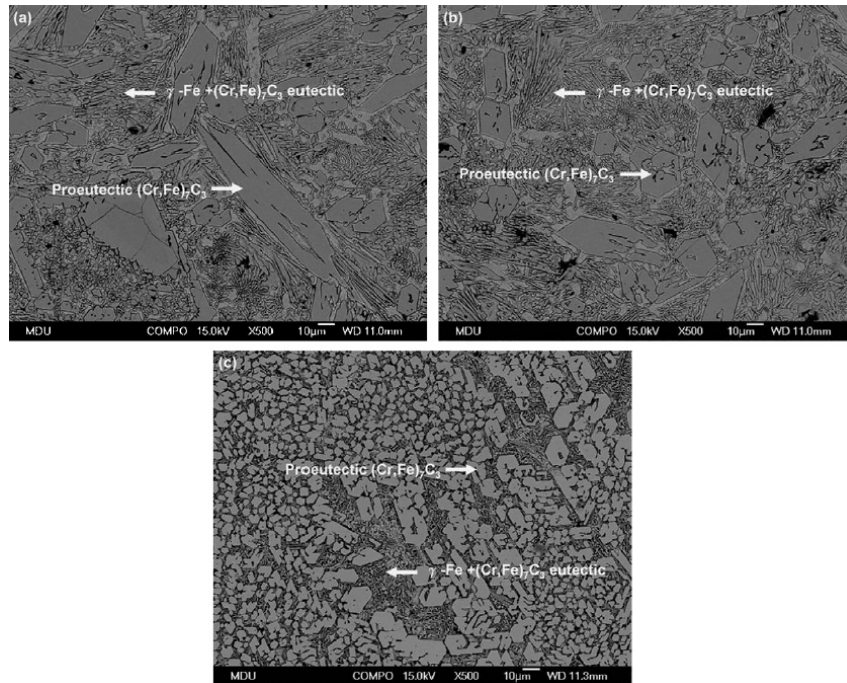


**Figure 16: SEM images of Fe-Cr-C claddings with C contents (a) 3.73 wt. % (b) 4.21 wt. % (c) 4.85 wt. % [18]**

Hardness test was conducted on these claddings. And it was quite clear that the specimen C, with the highest carbon content had the highest hardness value due to the large amounts of proeutectic carbides present in the microstructure. The hardness was also found to be inversely proportional to the size of the particles. Hence causing specimen C to have the highest hardness.

## **2.6 Abrasive Wear**

Abrasive wear is referred to as removal of material from a surface by a harder material impinging on or moving along the surface under load [26]. Certain groups of cast iron that have an excellent abrasion resistant, and are often desired in the mineral and mining industry. There are a number of mechanisms that influence abrasive wear. These mechanisms also decide the manner of material removal. The common abrasive wear mechanisms are microcutting, microploughing, microfatigue and microcracking as shown in Figure 17.

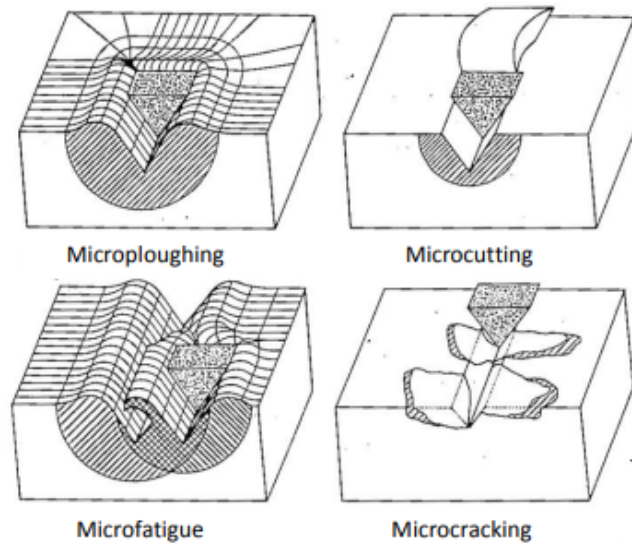


**Figure 17: Abrasive wear mechanisms**

M. Atabaki et al. conducted a study on comparing abrasive wear of HCCI and Hadfield steels. The results were compared using pin-on-disk wear test [28]. Microstructural analysis of HCCI showed that the retained austenite could not resist against abrasion. Carbide phase were shown to enhance wear rates. The low strength carbides could not resist strain caused by wear stress or pressing and shearing of the matrix in front of the abrasive [28]. Due to this, correlation was found between mass loss and matrix hardness after wear. Figure 18, shows that the mass loss is higher in HCCI due to the coarse carbide particles present. Increasing applied load, increased the mass loss of HCCI compared to Hadfield steels. The work hardening of the austenite by martensitic transformation could play an important role on the wear decrease [28].

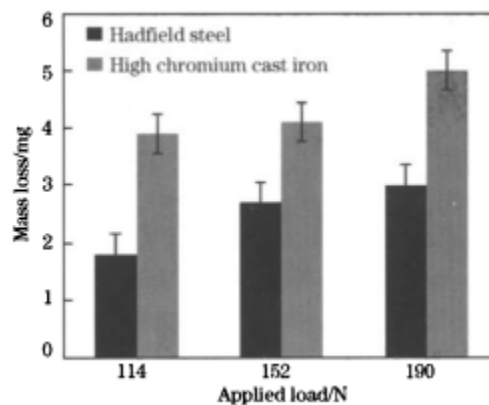


**Figure 18: Mass loss of pins under different loads [28].**

## **2.7 Critical Research Summary**

From our literature review we've defined what HCCI's are and the types of environments they are used in. The microstructure was looked at and we observed these eutectic carbides that give them their hard and excellent wear properties. The martensitic matrix was found to have the highest hardness value. But, a down fall with this was that the eutectic carbides would make the material too hard and brittle reducing its service lifetime. Improving toughness along with the hardness was one of the key objectives many of the researchers looked at.

Strong carbide forming elements are one way to try and solve this problem. Silicon was added to HCCI and with increasing Si content there was an increase in precipitation of secondary carbides which resulted an improvement in hardness and wear properties. Titanium was added to Hypereutectic HCCI and refinement of eutectic carbides took place. A key learning point from this was that it is not right to increase Ti content unlimitedly as it had a negative influence on the properties due to the drastic increase in TiC particle size. Addition of Nb to microstructure at different compositions saw changes to size of the NbC particle. Increasing content gave us hexagonal particles which improved the fracture toughness along with the other properties. The low solubility of Nb contributes to the refinement in the microstructure.

Heat treatment process which includes destabilization and tempering have proved to be beneficial in converting the austenite to martensitic matrix followed by some retained austenite on tempering. The retained austenite is known to have an impact on toughness in a positive manner. Different combinations of temperature and cooling conditions bring about different microstructural results. The composition of the HCCI also play an important role.

In Section 2.5, the reason for the high amounts of proeutectic carbides is because they start to appear first during the solidification process after which the eutectic structure formed around the boundaries of the proeutectic [18].

### 3.0 Methodology

During the course of this project, several experimental procedures had to be followed in order to try and achieve accurate results. The following section is broken down in to four main parts:

- (i) Sand Casting process where addition of Titanium and Niobium took place.
- (ii) Destabilization treatment and tempering of the A05 eutectic alloy samples.
- (iii) Cutting, mounting and polishing of samples.
- (iv) Hardness, microhardness, charpy, optical microscopy tests.

#### 3.1 Sand Casting

This is a metal casting process characterized by using sand as the mold material [19]. Firstly, sand of 30kgs is measured out in two buckets with 15kgs in each bucket, using a weighing scale. Sand is then poured into a sand mixer as shown in Figure 19. As the sand just starts to be mixed, 1 Litre of ‘Foseco Coolset 1 Resin’ is added from the top. This is used as bonding agent to transform the fine sand into a more moist binding structure to strengthen the sand when it goes into the mould. After the resin is added, the sand continues to mix for about 15-20 minutes.

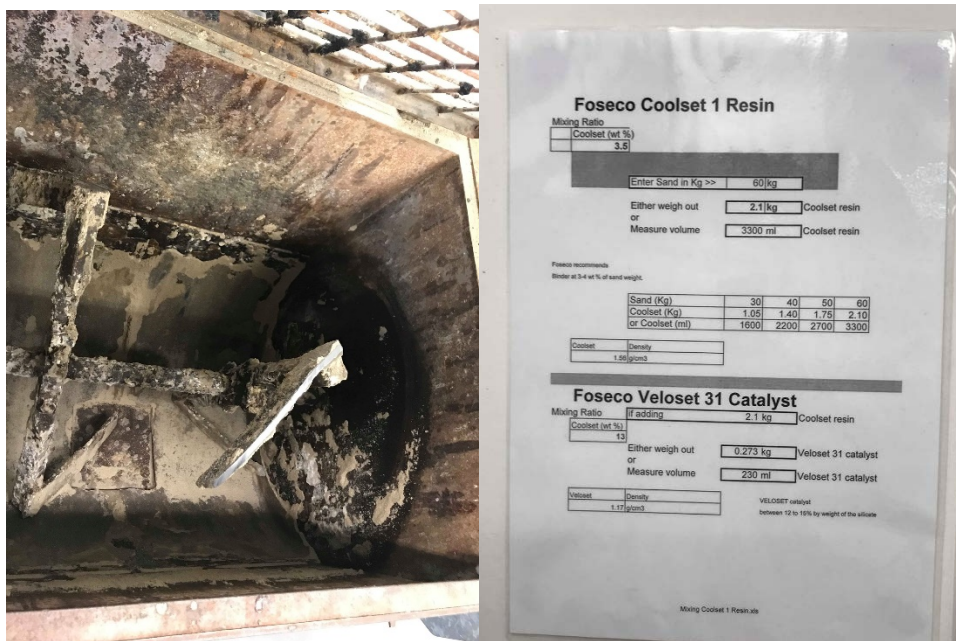
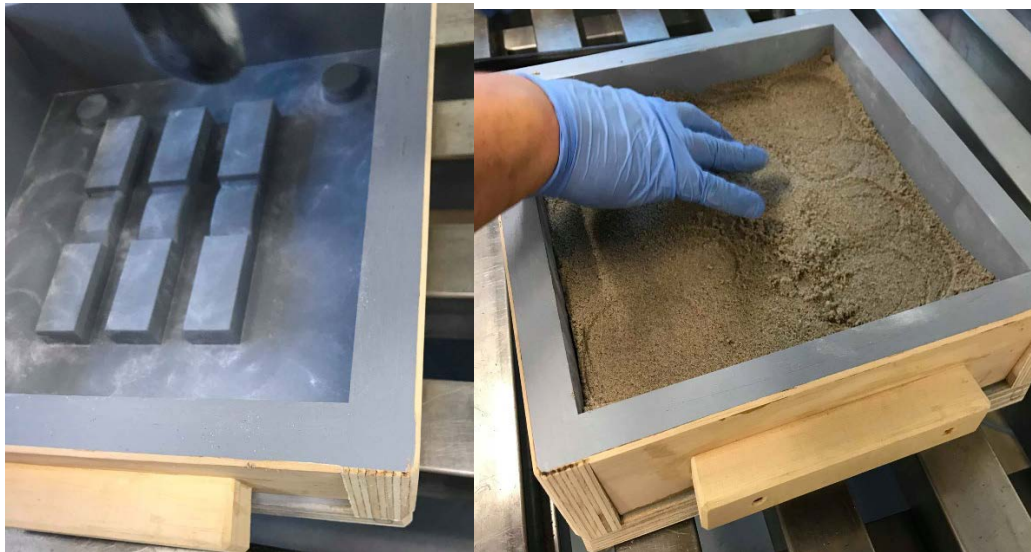


Figure 19: Sand Mixer & Coolset Resin

Figure 20, shows the sand mould that is being used. The mould shown, gives us six samples for each of the different Ti and Nb compositions. The mould is first powdered especially on the sides to make sure that the end product comes out smoothly from the mould. Filling of the sand into the



mould comprised of two stages. First, was to put the sand into the mould up to about half way. Using a flat head circular hammer, the sand was flattened out as shown in Figure 21. The process was repeated three-four times to make sure all the edges were flat and ensure the entire sand structure was moderately strong. The second stage was to put in more sand and fill it up to the brim. Our palms were used in this case to flatten the sand out. Eight holes at different locations on the surface of the sand mould were marked to allow  $CO_2$  gas to pass through the bottom of the mould. This is done to further harden the sand mixture giving it enough strength during the metal pouring process. Dimensional accuracy is known to be achieved using this process. The finished products are shown in Figure 22. The same procedure is followed for mould on the left. This mould goes on top, and from the big hole, is where the molten metal is poured in and separates into the six sample spaces. This process was repeated for addition of Ti and Nb at compositions of 0, 0.5, 1 & 2 wt. %.



**Figure 20: Sand Mould design**

**Figure 21: Sand levelled using flat head hammer**

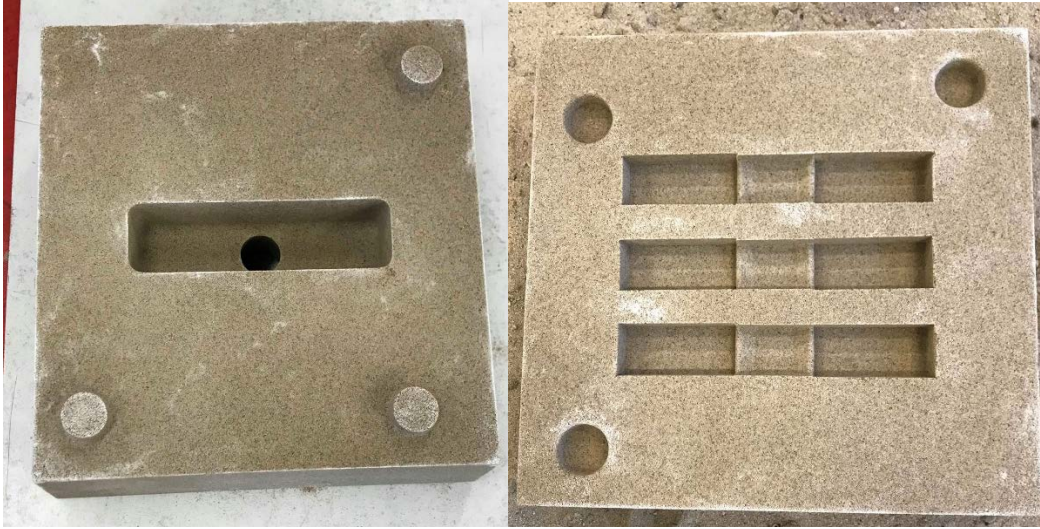


**Figure 22: Complete sand mould set**

### **3.2 Destabilization & Tempering Treatment**

A05 eutectic alloys were subjected to destabilization and tempering. The composition of this alloy has been previously mentioned in Section 1.2. The destabilization heat treatment processes for this alloy were to austenize these alloys at  $950^{\circ}\text{C}$ ,  $1020^{\circ}\text{C}$ ,  $1080^{\circ}\text{C}$ ,  $1130^{\circ}\text{C}$ ,  $1190^{\circ}\text{C}$  for 6 hours. Figure 23, shows these specimens placed in iron boxes half filled with sand. These were then later buried in a sand and coke mixture to prevent oxidation and decarburization.



**Figure 23: 3 samples placed for each temperature**

Once these samples were taken out of the furnace, they were allowed to air cool. This was then followed by tempering. The specimens were tempered at  $260^{\circ}\text{C}$ ,  $320^{\circ}\text{C}$ ,  $500^{\circ}\text{C}$ ,  $600^{\circ}\text{C}$  for 3 hours, respectively in order to observe and discuss the influence of tempering temperature on the properties and microstructure [2].

### **3.3 Cutting, Mounting, Polishing**

Once all these samples have been heat treated and sand casted, for testing purposes, these samples need to be cut to size, mounted and polished in order to view under the microscope or for other testing purposes. The samples are cut using a blade which is chosen according to standards that have been formulated by the blade company provider. The cutting machine has been represented in Figure 24(a). This is then followed by mounting where, PolyFast, a hot mounting resin is used to enclose the cut sample as shown in Figure 24 (b). Grinding and polishing then follows to get the observing area free of scratches. The polishing machine is shown in Figure 25(a) and the process includes three stages of polishing with three different sets of mats, refer Figure 25(b). Samples for optical microscopy were etched using a solution of 50ml 1 FeCl<sub>3</sub>, 20 ml of HCl, and 20 ml of ethanol. This solution attacks the preferentially the ferrous matrix leaving the carbides relatively unaffected, leading to a good contrast between carbides and matrix [20].

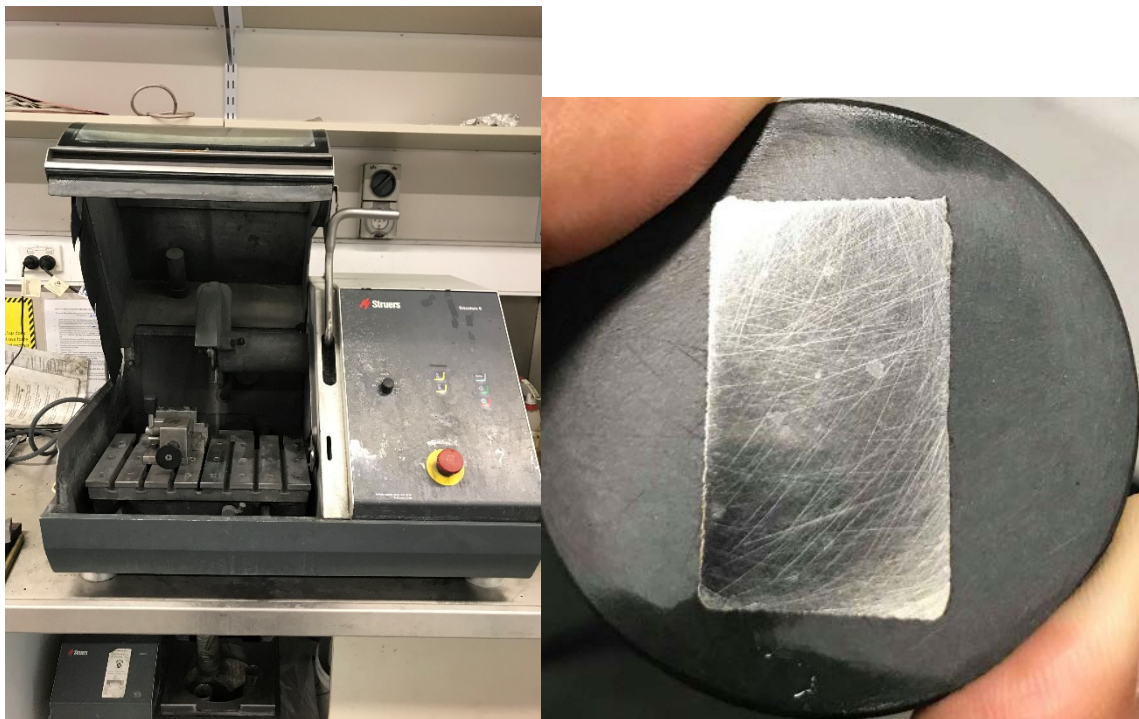


**Figure 24: (a) Cutting machine; (b) Mounted sample**



**Figure 25: (a) Polishing Machine & (b) Mats**

### **3.4 Testing Equipment**

Rockwell and Microhardness (HV0.3) testing was performed for both heat treated and sand casted samples. In order to measure the toughness, Charpy test equipment was used. The toughness measured in high chromium white irons using the Charpy test is very low and it is hard to distinguish the differences in toughness for various conditions [2]. Thus, in the present work, the impact toughness was determined by using un-notched Charpy size specimens. The Charpy test was only conducted on heat treated and tempered samples. Optical Microscope was used to view and analyze the microstructure of all the specimens. Figure 26 shows the Vickers and Optical Microscopy testing equipment's used respectively. Figure 27 shows the Rockwell and Charpy test equipment's. On the mounted sample (Figure 24 (b)), five different spots were chosen to measure the hardness values. These values were then averaged to obtain the overall hardness of the material.

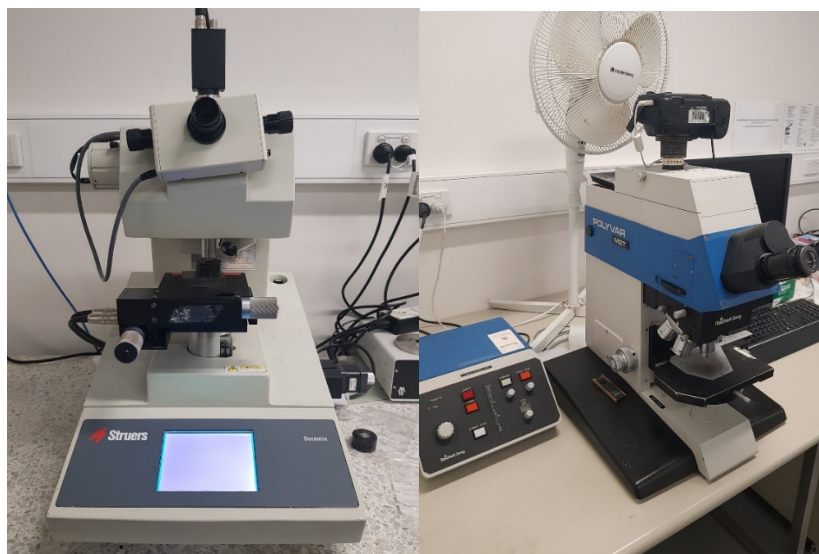


**Figure 26: Vickers Hardness & OM**



Figure 27: Rockwell & Charpy Test Equipment

### 3.5 Weight % Calculation

For about 3-3.5 kg's of A05 alloy and different wt. % compositions (0.5, 1.0, 2.0), the amount of Titanium or Niobium to be added to the melt had to be calculated. The following formula was used:

$$\frac{W_{Ti\ or\ Nb}}{W_{Ti\ or\ Nb} + W_{A05}} = wt.\ \% \ compositions$$

$W_{Ti\ or\ Nb}$  Is the value that is needed to be found. Table 5 below gives the amount of Titanium required to be added for each of the compositions.

Table 5: Weight of Titanium Required

Wt. % Composition	Total Weight of A05 (kg)	Total Weight of Titanium (gms)
0.5	3.355	16.85
1.0	3.420	34.50
2.0	3.300	67.30

## 4.0 Results

They were mainly two sets of results that were obtained during the course of the experiments. First being, destabilization and tempering treatments of the A05 alloy. Secondly, the addition of Ti and Nb to the A05 alloy at different compositions through sand casting.

### 4.1 Heat Treatment Results

With the heat treated samples, the impact toughness, Vickers and Rockwell hardness testing was done. Microstructure was also critically analyzed.

#### 4.1.1 Impact Toughness

Variations in impact toughness at different temperatures have been shown in Figure 28 and 29. The cross section of the specimen was found to be 1.25cm x 1.20cm. This was required as to find the toughness in  $J/cm^2$ . Considering the destabilization treatment first, we see that as the temperature increases from 950<sup>o</sup> to 1190<sup>o</sup>C, the impact toughness keeps increasing. Only at 950<sup>o</sup> the toughness value is equal to the as-cast state. This confirms the fact that destabilization treatment can significantly improve the toughness of this alloy. On the other hand, looking at the tempering graph, we see that the maximum value of toughness is obtained at 260<sup>o</sup>C. Above this temperature the values start to drop and it gets even lower than the un-tempered value for temperatures above 500<sup>o</sup>C.

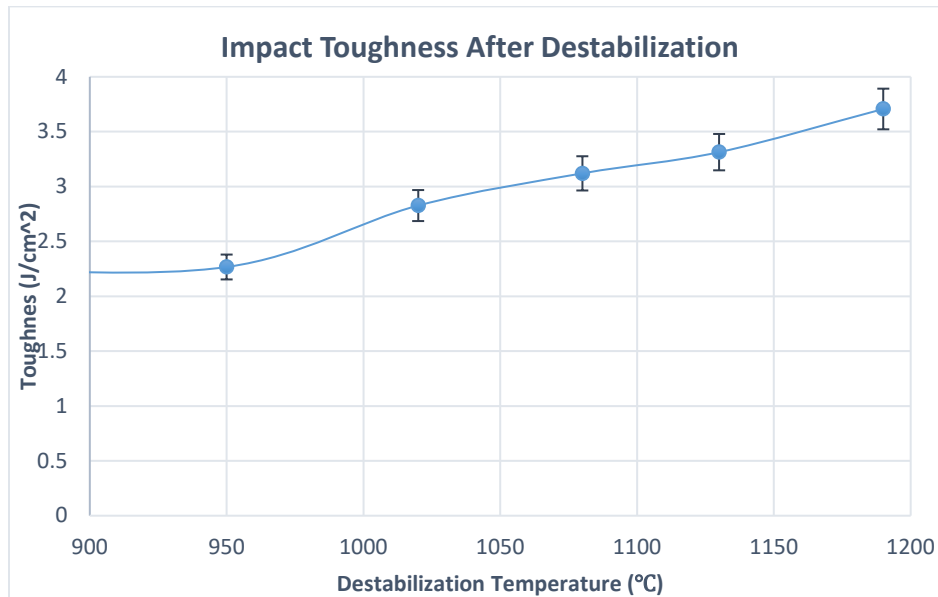


Figure 28: Variation of Impact Energy with Destabilization Temperatures

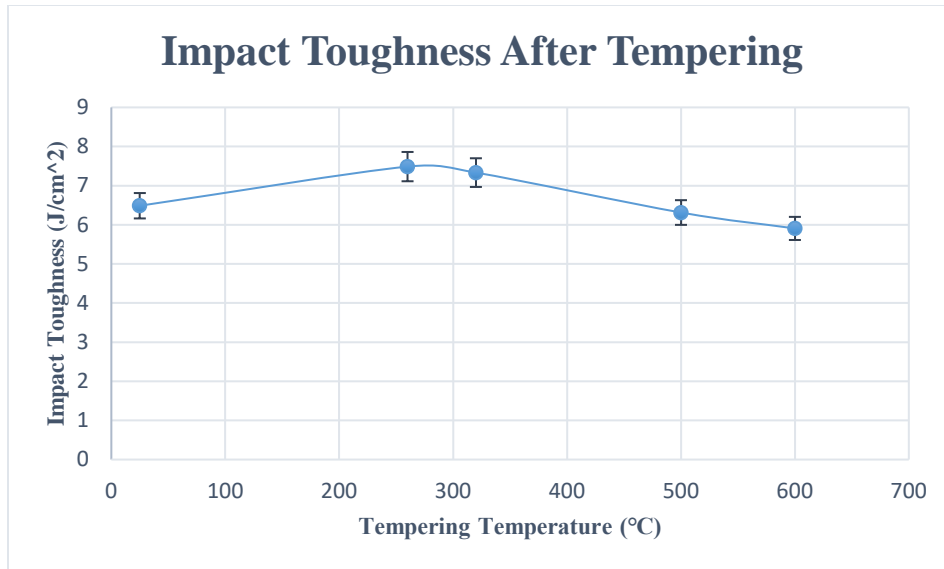


Figure 29: Variation of Impact Energy with Tempering Temperatures

#### 4.1.2 Vickers & Rockwell Hardness

Figure 30 represents the Vickers hardness after destabilization. We observe that as the temperature is increased to 950<sup>0</sup>C, there is a sharp increase in HV value from approximately 475HV (as-cast) to 700.5HV. But, as the temperature increases beyond this, the hardness values start to drop but they are still found to be higher than 475HV. Considering Figure 31, the hardness value decreases from the un-tempered state between temperatures of 260-320<sup>0</sup>C. As the temperature reaches 500<sup>0</sup>C or more, the hardness values start to rise and it even higher than the un-tempered condition. This increase in hardness is due to the secondary hardening taking place.

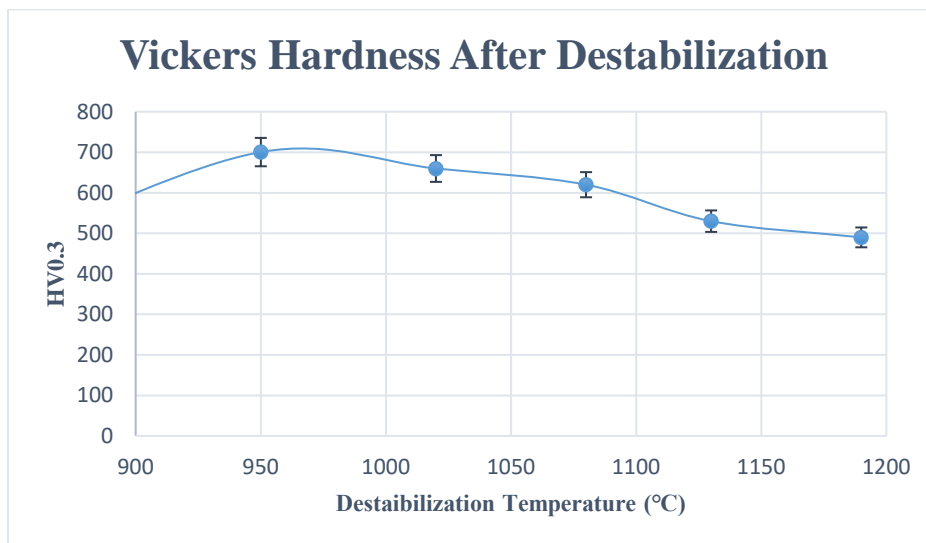
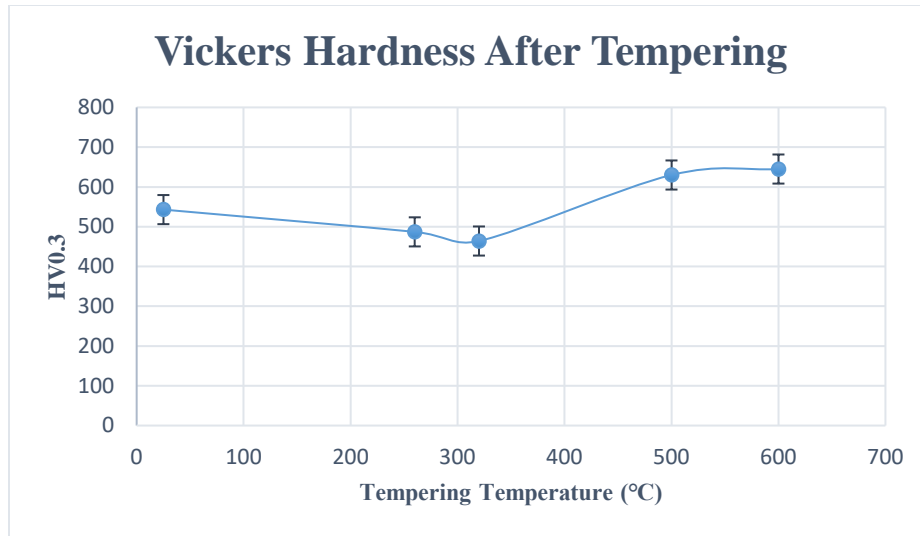
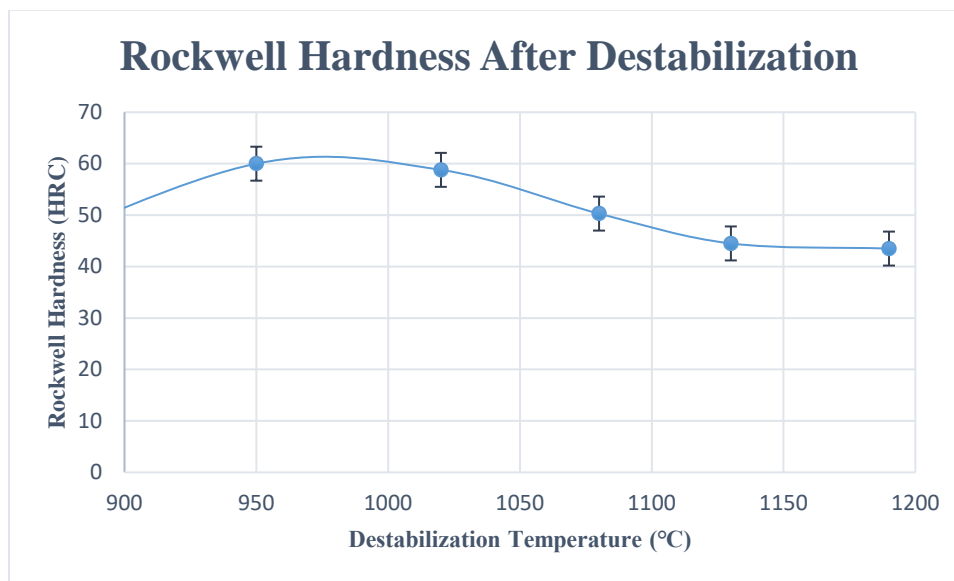


Figure 30: Variation of Vickers Hardness with Destabilization Temperature.



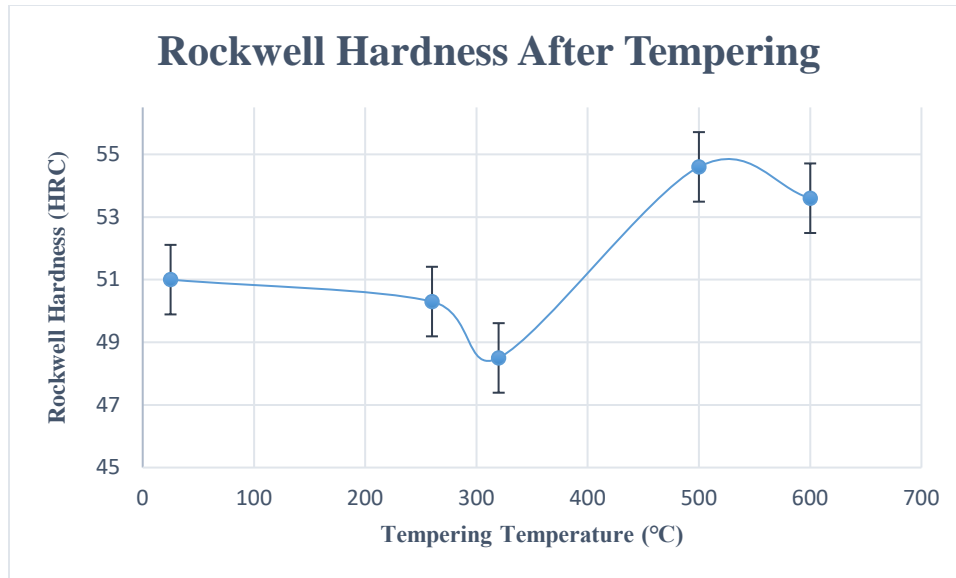
**Figure 31: Variation of Vickers Hardness with Tempering Temperature.**

Figure 32 & 33 give us the Rockwell hardness (HRC) after destabilization and tempering respectively. With regards to Figure 32, the trend observed is very similar to the Vickers hardness results. However, Figure 33 see a slight drop in hardness value at higher temperatures but this is still higher than the un-tempered state.



**Figure 32: Variation in Rockwell Hardness with Destabilization Temperature.**





**Figure 33: Variation in Rockwell Hardness with Tempering Temperature.**

#### 4.1.3 Microstructure

As mentioned before in previous sections, a hypoeutectic HCCI would generally consider of austenitic dendrites with a eutectic mixture of austenite and carbides and on heating would generally transform to martensite. For the specimens used in our case, transformation to martensite is observed. Figure 34(a) & (b) respectively show images of microstructure in the as-cast and destabilization at  $1130^{\circ}\text{C}$ . We see that with increase in temperature small particles start to form. These are nothing but the precipitation of secondary carbides. These carbides grow within regions where the austenite has transformed into martensite. As the temperature kept increasing, the amount of secondary carbides and transformed martensite started to decrease. Past research has shown that both the eutectic and secondary carbides are  $M_7C_3$  type carbides [2]. Tempering does change the microstructure morphology of white cast iron to an extent. We see that the dendritic carbides have actually become a little thicker rather than thin blade-like structures. At higher temperatures, precipitation of secondary carbides is observed within the structure as marked in Figure 35. It shows the microstructure of the tempered specimen at  $600^{\circ}\text{C}$  after being destabilized at  $1130^{\circ}\text{C}$  for 6 hours. Chemical composition and crystal structure of the secondary carbides as well as TEM analysis were not investigated.

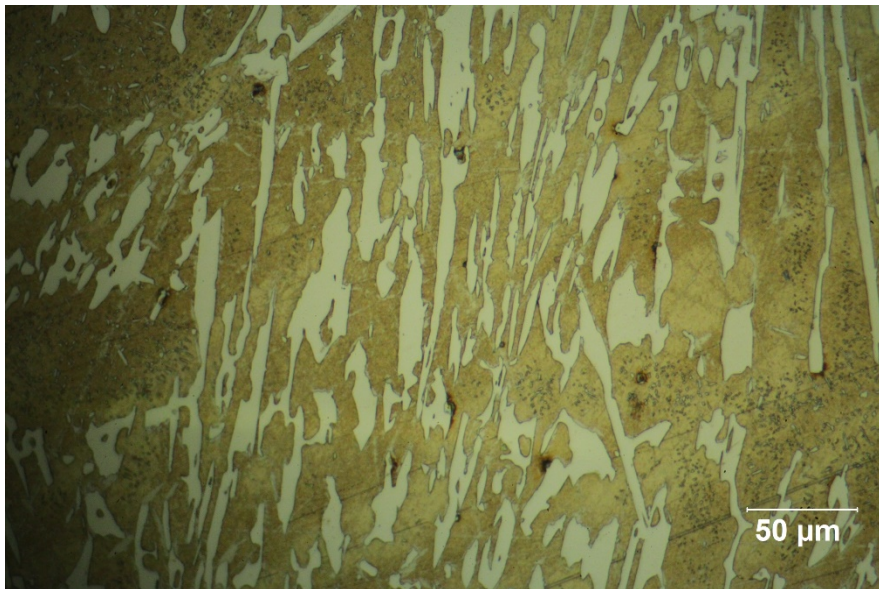
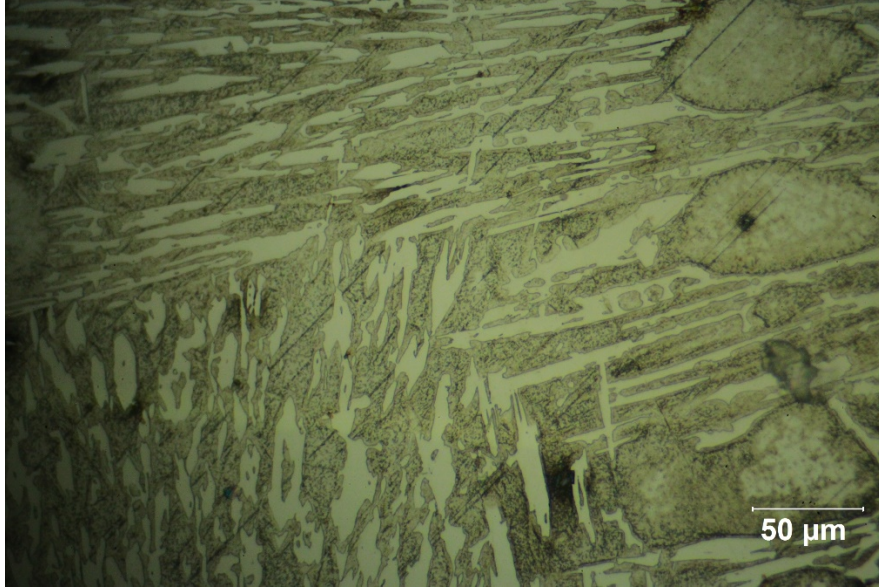


**Figure 34: (a) As-cast state; (b) Destabilization treatment at 1130°C for 6h**

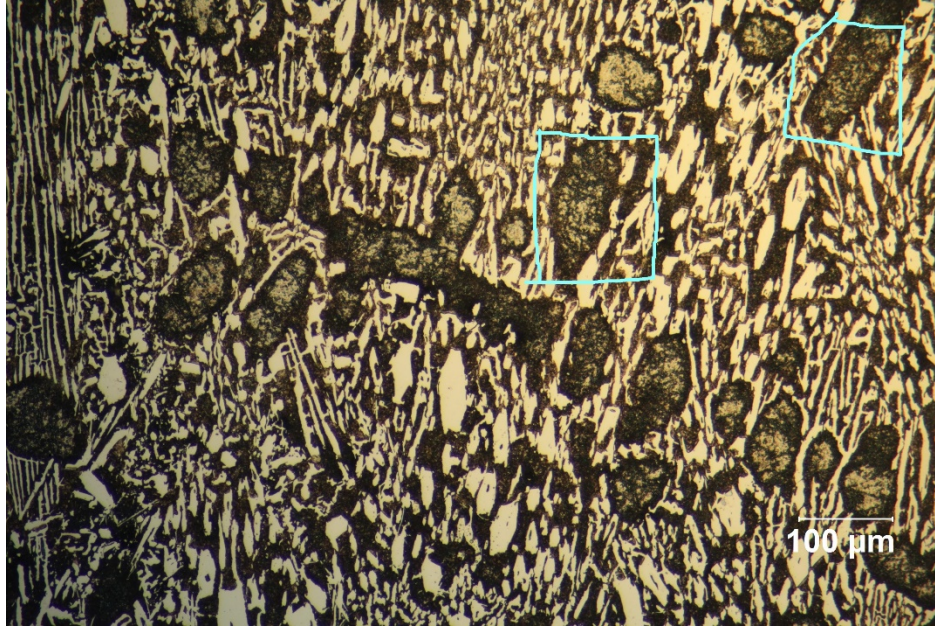


Figure 35: Tempered specimen at 600°C

## 4.2 Titanium Addition Results

To the A05 alloy melt, during the casting process, compositions of 0.5, 1.0 & 2.0% Ti was added. Microstructural, Rockwell and Vickers Hardness analysis were conducted.

### 4.2.1 Vickers & Rockwell Hardness

Figure 36(a) and (b) represent the Vickers and Rockwell hardness at different Titanium compositions respectively. As the Ti composition increases, we observe an increase in both hardness values. But this only occurs up to 1 wt. % Ti, after which further addition leads to a decrease in hardness. This similar trend has been observed in previous studies (Refer Section 2.3.2.1) and it goes onto say that it is not right to increase the Ti content unlimitedly as it has a negative influence on the properties. This is commonly attributed due to the refinement of the  $M_7C_3$  carbides as their volume fraction decreases, reducing their hardness.

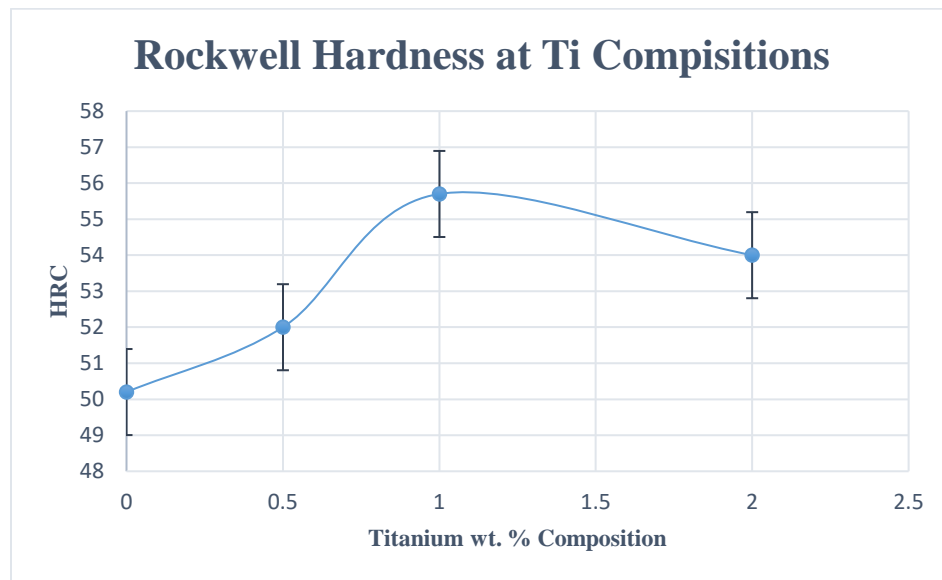
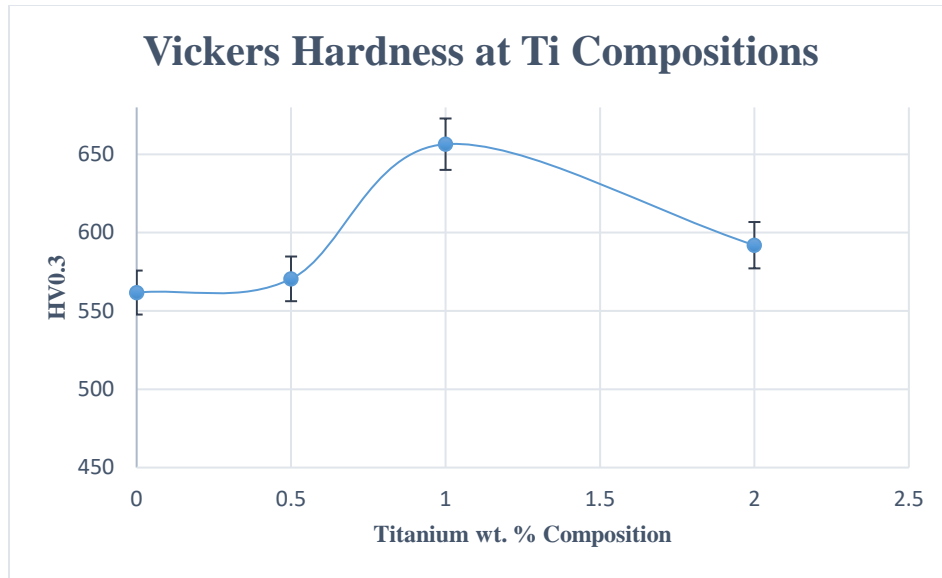


Figure 36: Titanium addition (a) Vickers Hardness; (b) Rockwell Hardness

### 4.3 Niobium Addition Results

To the A05 alloy melt, during the casting process, compositions of 0.5, 1.0 & 2.0% Nb was added. Microstructural, Rockwell and Vickers Hardness analysis were conducted.

#### 4.3.1 Vickers & Rockwell Hardness

Niobium does not have a great, but it is still a noticeable effect on this A05 alloy. As the composition increases we see the Vickers hardness rising from 561HV to about 570HV. This trend is also observed with the Rockwell Hardness. Figure 37 (a) and (b) represents the Vickers and

Rockwell hardness respectively. These results have found to be similar to what has been obtained in previous works. The structural refinement and increased NbC phase attributes to these results.

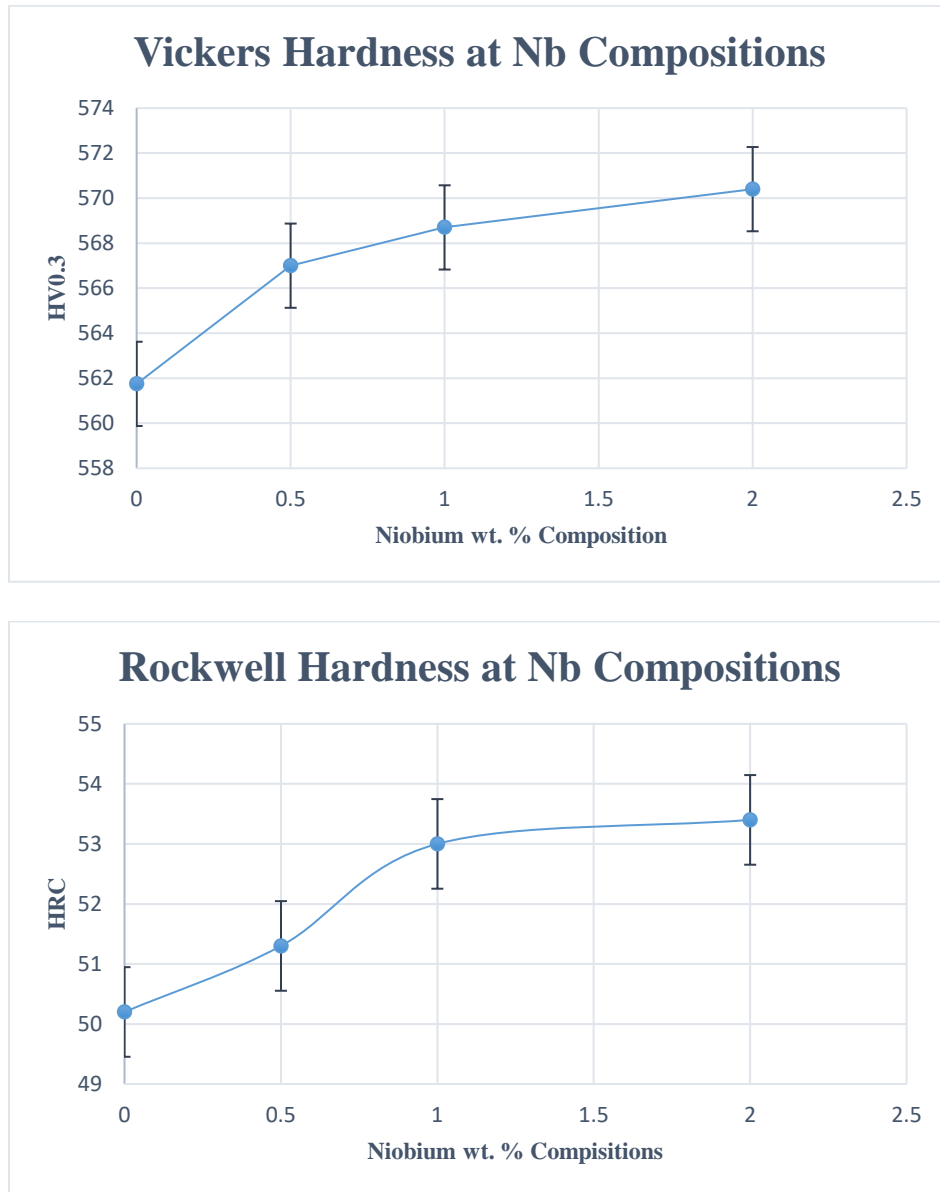


**Figure 37: Niobium addition (a) Vickers Hardness; (b) Rockwell Hardness**

## 5.0 Discussion

### 5.1 Heat Treatment – Impact Toughness

As mentioned in previous sections, HCCI are known for their excellent wear and abrasion resistance. Their microstructure primarily consists of large eutectic carbides of  $M_7C_3$  that are really hard and brittle. These application is mainly in the mining industry or slurry pumps where significant impact is not involved. Therefore, this does limit its application and cannot be used in applications that require high impact. The HCCI have very low toughness and improvement of this property would significantly improve service life [2]. Martensite is known for their hardness, whereas austenite is associated with fracture toughness. To improve the toughness, retaining the austenite is important. Greater the increase in retained austenite, more improved is the fracture toughness. At higher temperatures transformation to martensite occurs. This transformation causes dissipation of energy from the stress-induced martensitic transformation [2]. But, it is important to find the optimum amount of retained austenite as, if the amount is too high the toughness will not improve. Similarly, if the retained austenite is less, the dissipation energy will be small and not have a significant impact on improving toughness. Many previous studies have shown that the improved amount of retained austenite with increasing temperature had little effect on the fracture toughness. But results from Section 4.1.1 show that toughness increases with increasing destabilization temperature. Tempering also had an impact on the toughness. The highest toughness value is obtained between 260<sup>0</sup> and 320<sup>0</sup>C due to the release of residual stresses. As temperature rises above 500<sup>0</sup>C, the decomposition of retained austenite leads to a decrease in toughness [2].

### 5.2 Heat Treatment – Hardness

It is known that, at high destabilization temperatures the toughness is improved and this is generally accompanied with the decrease in hardness, which is not desirable. Figure 27 shows that as the temperature increases the hardness values constantly drops, but, this is still higher than the as-cast value. Past research has shown that austenite can actually have a positive impact on the abrasion resistance [22]. Eutectic carbides play a major role in improving wear resistance. They are equally supported by the austenite matrix through work hardening and stress-induced martensitic transformation [2]. In the case of high abrasion resistance, the hard eutectic abrasive particles work harden the austenite by stress-induced transformation. External stress during service provides a mean to determine whether the austenite will provide good support to carbides. High

mechanical stability of retained austenite has found to have a negative impact on the abrasion resistance. Section 2.5 says that increase in carbon content changed the size of the proeutectic carbides and increased hardness thereby increasing mechanical stability of the retained austenite. The destabilization treatment has found to improve the abrasion resistance through the mechanism of reducing the carbon content in the alloy which would in turn reduce the mechanical stability. With lowering carbon content, studies have concluded that as long as the presence of pearlite and bainite are avoided, high abrasion resistance would be obtained [2]. Optical microscopy images from Figure 31 (b) confirm no indication of pearlite and bainite ensuring good abrasion resistance of alloys. Thus, low carbon white cast irons with high destabilization temperature could prove one of the best materials for conditions involving high impact and abrasion [2].

### **5.3 Niobium Addition**

Addition of Niobium has found to be bring about changes in the properties. As the composition is increased up to about 2%, the hardness values do go up but not significantly. Figure 38, 39 and 40 below compares the microstructure of the alloy at 0 wt. %, 0.5 wt. % and 2.0 wt. % Nb respectively. At 0 wt. % we only observe the austenite matrix along with the  $M_7C_3$  carbides. Whereas at 2 wt. %, dispersion of NbC particles are observed in the carbide. The number of NbC particles observed at 2 wt. % are not quite as high as discussed in literature (Section 2.3.3.1). This could be due to the fact that the specimens we are dealing with has a completely different composition to that shown in the literature. MC type carbides are formed within the microstructure due to the low solubility of Nb in the austenite and  $M_7C_3$  carbides [13]. At 0.5 wt. % Nb, the NbC particles are difficult to observe. In general, the shape observed of these carbides are more petal-like or rod-like structures (marked in Figure 39). As solidification starts from the melt, the primary austenite  $\gamma$ -phase is the first to solidify. Niobium, carbon and chromium are known to have low solubility in austenite and so as the temperature continues to drop, these elements accumulated in front of the progressing solid-liquid interface [13]. In areas enriched with Niobium, the NbC carbides are formed within the eutectic carbides. This blocks further growth of the  $\gamma$ -phase. At 2 wt. % Nb, there are a few NbC particles that have refined in size to being more hexagonal shape giving its slight improvement in hardness. This is because here the NbC are first to solidify from the melt. With increased Nb content, it leads to depletion of carbon in the liquid, which in-turn results in reduction of  $M_7C_3$  carbides. The ever so slight increase in the hardness is understood due to the fact that the decrease in the eutectic carbides, could actually contributes greatly to the fracture

toughness of the alloy. The following figures have been marked showing the formation of the NbC carbides in the microstructure.

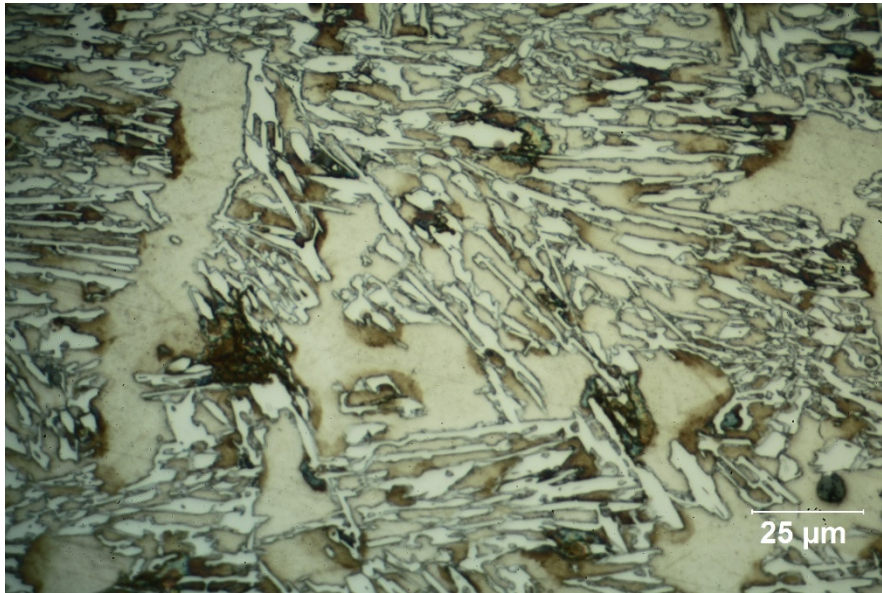


**Figure 38: A05 alloy with 0 wt. % Nb**

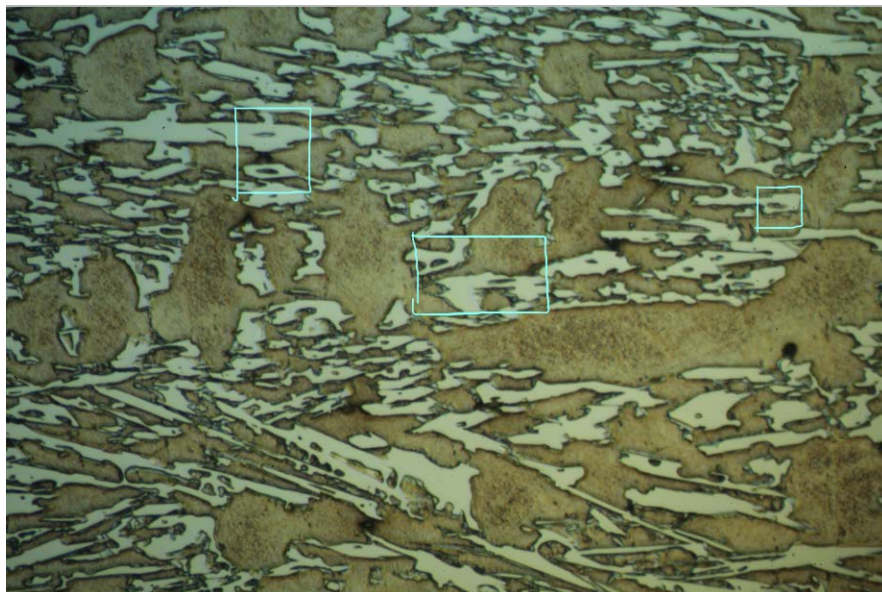


**Figure 39: A05 alloy with 0.5 wt. % Nb**



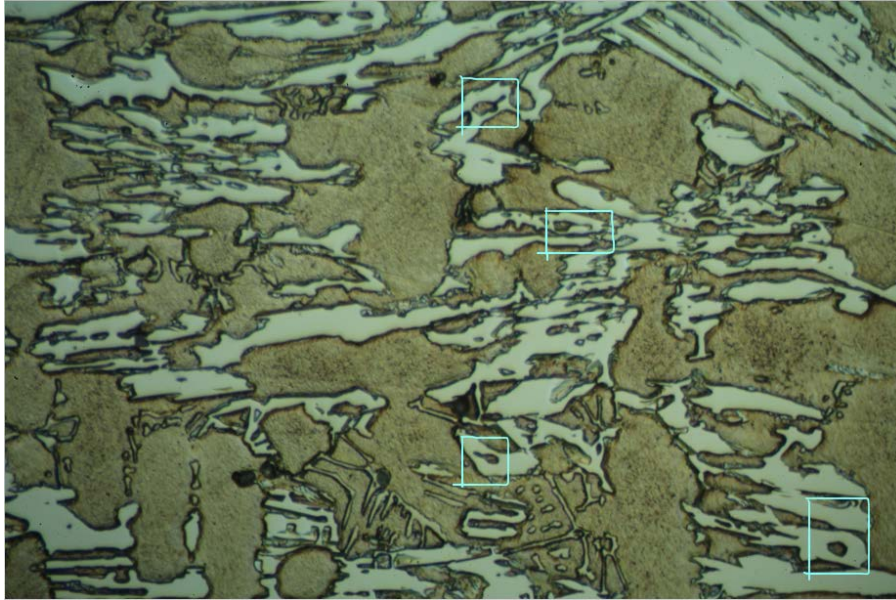
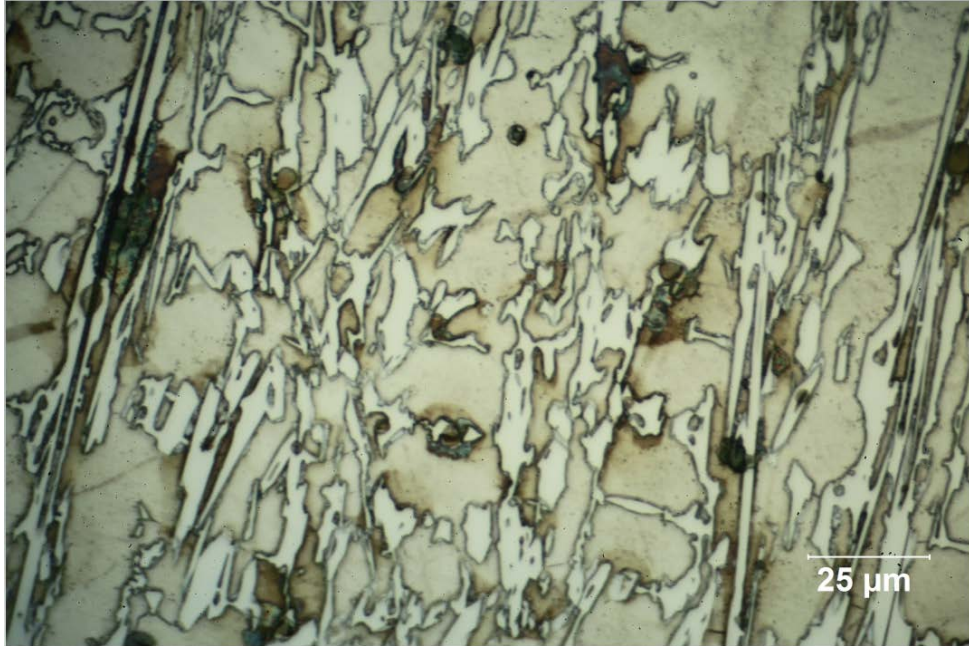


Figure 40: A05 alloy with 2.0 wt. % Nb

#### 5.4 Titanium Addition

Titanium when added to the melt of the alloy, is expected to form TiC carbides which are expected to alter the microstructure and properties. From Section 4.2, plots of Vickers and Rockwell hardness show that the hardness constantly rises with increasing Ti composition up to 1%. After this, the hardness is seen to fall. With these results obtained, we would expect to see the formation of TiC particles along with refinement of primary  $M_7C_3$  carbides. Some of the research have also concluded that TiC can effectively act as a heterogeneous nuclei. However, in this current study, no such evidence of dendrite refinement was observed but it is believed to have still occurred [24]. Addition at 2 wt. % (marked in Figure 40) revealed presence of really small particles that were present in the austenite matrix. Studies by A. Bedolla-Jacuinde et al. have also shown the presence of these particles. On further investigation using SEM and EDS, these particles he had found them to be Ti-rich and maybe a carbide or carbonitride [24]. With increasing Ti content, the TiC particles could promote higher austenite volume fraction. His analysis on the carbide volume fraction showed that it kept decreasing with increasing TiC particles as it would promote austenite precipitation. Figure 41, 42 and 43 below represent the microstructure at the different wt. % compositions of Titanium.



**Figure 41: A05 alloy with 0 wt. % Ti**

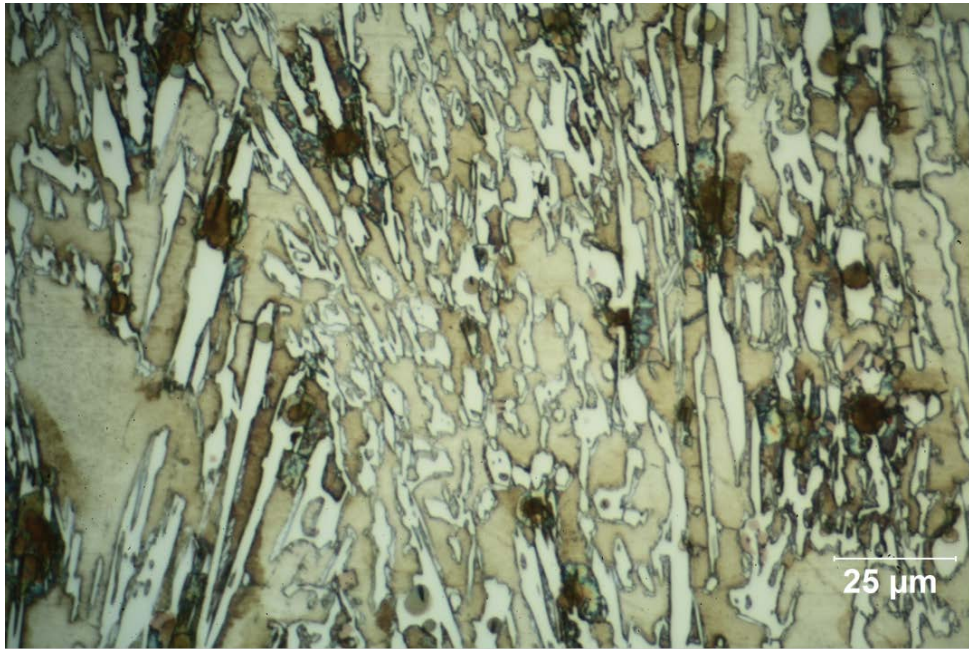


**Figure 42: A05 alloy with 1 wt. % Ti**

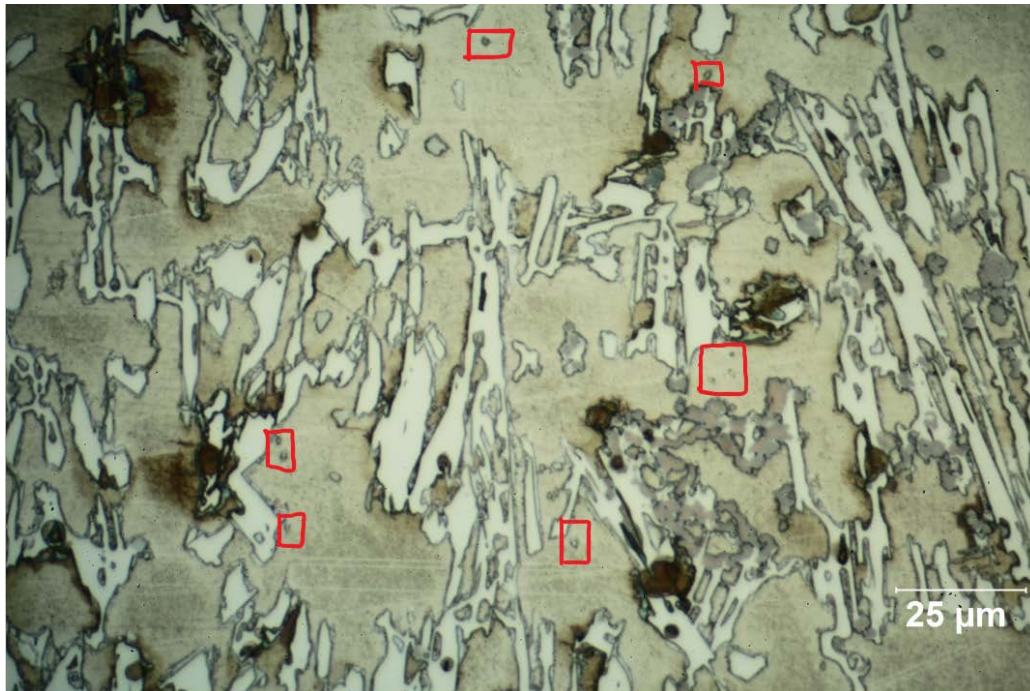


**Figure 43: A05 alloy with 2 wt. % Ti**

There could be several reasons as to why we do not observe a prominent change in microstructure with the Ti addition. Firstly, each research work is different from the other. Not every study deals with the same kind of alloy. Specimens used in experiments can have different compositions of C and Cr in them and so addition and formation of carbide forming elements in the microstructure can vary. Secondly, the casting process might have not been well followed. Each SCF has a different melting temperature and so if the temperature is not high enough, the results obtained would not be accurate. Observations only using the optical microscope is not enough in this case. Usage of the SEM or EDS would help us understand and differentiate the particles much better. Solidification of the melt might have led to formation of complex Fe-Ti-Cr structure which makes it difficult to find TiC.

## 6.0 Conclusions

Keeping in mind the primary aims outlined in Section 1.1, the following conclusions can be drawn based on the discussion of results.

Varying conditions of heat treatment brought about different properties in the A05 alloy. With increasing destabilization temperature impact toughness was found to increase. Retained austenite was found to play an important role. Greater the increase in retained austenite greater the toughness. Stress induced martensitic transformation led to dissipation of energy which is crucial in assessing the amount of austenite retained. Tempering showed us that the at lower temperatures maximum toughness was obtained but as the temperature increased to more than  $500^{\circ}\text{C}$ , toughness value dropped due to precipitation of secondary carbides. Hardness values were seen to drop with increasing destabilization temperature. But, these values were still higher than the as-cast state which shows improvement in hardness. Due to this improvement in hardness, the abrasion resistance properties have also improved with increasing temperature.

SCF elements such as Nb and Ti were added to the melt. With increasing Nb composition, the hardness values did go up, but not by much. The number of dispersed NbC particles are not quite as high as literature suggests. But as Nb composition increases, these particles sizes are found contributing to the slight improvement in hardness. Also, the increasing NbC is said to deplete the carbon content and the carbides hence could lead to improvement in toughness.

Ti showed us that the hardness increased quite a lot with increasing concentration up to 1%, beyond which, the hardness began to drop. The TiC particles observed were really small and present in the austenite matrix rather than the carbide. Studies have shown this reduces the volume fraction of the carbide by increasing precipitation of the austenite matrix. Improved experimental techniques would be required to obtain more accurate results and help enhance our understanding.

## 7.0 Recommendations

Projects involving experiments that are long and involving lot of stages, can often go wrong at some point and lead to inaccurate results. This was noticed during the sand casting process during the addition of Ti and Nb. Some of the improvements that could be made are as follows:

- Usage of SEM and EDS devices to obtain more detailed analysis of microstructure and different sized particles observed to further strengthen our understanding;
- Recommended to cast  $40^{\circ}C$  above the flow of the metal to allow it to be thoroughly molten;
- Porosity can be prevented by controlling sprue size- making sure it as heavy as the heaviest section of the casting;
- Protecting the metal from oxidation and absorbing unwanted gases by using protective inert gases like Argon etc. [25]
- Accurate temperature is important to obtain a good casting. As if it is too hot or cold, could lead to porosity or freezing of the metal in the casting, respectively. Always recommended to keep a close eye on the temperature value.

For the Ti and Nb samples only hardness test was done. Conducting charpy test along with wear resistance testing would give us more results and deeper understanding to compare our results with that obtained from past researches. Calculating carbide volume fraction helps us accurately understand its variation with increasing or decreasing composition. Using phase diagrams, to help us calculate solubility of Ti or Nb in melt at the liquidus temperature, can help us determine whether TiC or NbC will be formed before the precipitation of primary carbides. Literature has shown as that, heat treating HCCI that already have strong carbide forming elements present in them can bring about much better improvement in properties. Since, we solely focused on SCF elements and heat treatment separately, it would be recommended to try combinations of these processes.

## 8.0 References

- [1]"High Chromium Cast Iron: Part One :: Total Materia Article", *Totalmateria.com*, 2019. [Online]. Available: <https://www.totalmateria.com/page.aspx?ID=CheckArticle&site=kts&NM=497>. [Accessed: 21- May- 2019]
- [2]M. Zhang, P. Kelly and J. Gates, "The effect of heat treatment on the toughness, hardness and microstructure of low carbon white cast irons", *Journal of Material Sciences*, p. All, 2001.
- [3]C. Foulke, "The effect of chromium on white cast iron", IOWA State University, 1930.
- [4]E. Karantzalis, A. Lekatou and H. Mavros, "Microstructure and properties of high chromium cast irons: effect of heat treatments and alloying additions", *International Journal of Cast Metals Research*, vol. 22, no. 6, pp. 448-456, 2009.
- [5]"High Chromium Cast Iron: Part Two :: Total Materia Article", *Totalmateria.com*, 2019. [Online]. Available: <https://www.totalmateria.com/page.aspx?ID=CheckArticle&site=kts&NM=500>. [Accessed: 22- May- 2019]
- [6]W. Fairhurst and K. Rohrig, "Abrasion-Resistant High-Chromium White Cast Irons", *Foundry Trade Journal*, vol. 136, 1974.
- [7]G. Laird, R. Gundlach and K. Rohrig, "Abrasion-Resistant Cast Iron Handbook", *American Foundry Society*, 2000.
- [8]"Cast iron - tec-science", *tec-science*, 2019. [Online]. Available: [https://www.tec-science.com/material-science/iron-carbon-phase-diagram/cast-iron/#Cast\\_iron](https://www.tec-science.com/material-science/iron-carbon-phase-diagram/cast-iron/#Cast_iron). [Accessed: 23- May- 2019].
- [9]"Alloying Element - an overview | ScienceDirect Topics", *Sciencedirect.com*, 2019. [Online]. Available: <https://www.sciencedirect.com/topics/engineering/alloying-element>. [Accessed: 23- May- 2019].
- [10]J. Lai, Q. Pan, Y. Sun and C. Xiao, "Effect of Si Content on the Microstructure and Wear Resistance of High Chromium Cast Iron", *ISIJ International*, vol. 58, no. 8, pp. 1532-1537, 2018. Available: 10.2355/isijinternational.isijint-2018-099.
- [11]X. Zhi, J. Xing, H. Fu and Y. Gao, "Effect of titanium on the as-cast microstructure of hypereutectic high chromium cast iron", *Materials Characterization*, vol. 59, no. 9, pp. 1221-1226, 2008. Available: 10.1016/j.matchar.2007.10.010.
- [12]D. Kopyciński, E. Guzik, D. Siekaniec and A. Szczęsny, "The Effect of Addition of Titanium on The Structure and Properties of High Chromium Cast Iron", *Archives of Foundry Engineering*, vol. 15, no. 3, pp. 35-38, 2015. Available: 10.1515/afe-2015-0055.
- [13]M. Filipovic, Z. Kamberovic, M. Korac and B. Jordovic, "Effect of Niobium and Vanadium Additions on the As-Cast Microstructure and Properties of Hypoeutectic Fe–Cr–C Alloy", *ISIJ International*, vol. 53, no. 12, pp. 2160-2166, 2013. Available: 10.2355/isijinternational.53.2160.
- [14]Z. Zhiguo, Y. Chengkai, Z. Peng and L. Wei, "Microstructure and wear resistance of high chromium cast iron containing niobium", vol. 11, no. 3, 2014. [Accessed 24 May 2019].
- [15]L. Keen, "The Effect of Tempering on Abrasion and Chipping of White Irons", Undergraduate, University of Queensland, 2012.

- [16]"Tempering (metallurgy)", *En.wikipedia.org*, 2019. [Online]. Available: [https://en.wikipedia.org/wiki/Tempering\\_\(metallurgy\)](https://en.wikipedia.org/wiki/Tempering_(metallurgy)). [Accessed: 25- May- 2019].
- [17]H. Gasan and F. Erturk, "Effects of a Destabilization Heat Treatment on the Microstructure and Abrasive Wear Behavior of High-Chromium White Cast Iron Investigated Using Different Characterization Techniques", *Metallurgical and Materials Transactions A*, vol. 44, no. 11, pp. 4993-5005, 2013. Available: 10.1007/s11661-013-1851-3.
- [18]C. Chang, C. Lin, C. Hsieh, J. Chen, C. Fan and W. Wu, "Effect of carbon content on microstructural characteristics of the hypereutectic Fe–Cr–C claddings", *Materials Chemistry and Physics*, vol. 117, no. 1, pp. 257-261, 2009. Available: 10.1016/j.matchemphys.2009.05.052.
- [19]"Sand casting", *En.wikipedia.org*, 2019. [Online]. Available: [https://en.wikipedia.org/wiki/Sand\\_casting](https://en.wikipedia.org/wiki/Sand_casting). [Accessed: 26- May- 2019].
- [20]R. Chung, X. Tang, D. Li, B. Hinckley and K. Dolman, "Microstructure refinement of hypereutectic high Cr cast irons using hard carbide-forming elements for improved wear resistance", *Wear*, vol. 301, no. 1-2, pp. 695-706, 2013. Available: 10.1016/j.wear.2013.01.079.
- [21]I. Sare and B. Arnold, "The influence of heat treatment on the high-stress abrasion resistance and fracture toughness of alloy white cast irons", *Metallurgical and Materials Transactions A*, vol. 26, no. 7, pp. 1785-1793, 1995. Available: 10.1007/bf02670766.
- [22]A. Bedolla-Jacuide, L. Arias and B. Hernández, "Kinetics of Secondary Carbides Precipitation in a High-Chromium White Iron", *Journal of Materials Engineering and Performance*, vol. 12, no. 4, pp. 371-382, 2003. Available: 10.1361/105994903770342881.
- [23]M. Filipovic, Z. Kamberovic, M. Korac and Z. Andic, "WEAR RESISTANCE AND DYNAMIC FRACTURE TOUGHNESS OF HYPOEUTECTIC HIGH-CHROMIUM WHITE CAST IRON ALLOYED WITH NIOBIUM AND VANADIUM", no. 1580-2949, 2013. Available: <http://mit.imt.si/Revija/izvodi/mit143/filipovic.pdf>. [Accessed 28 May 2019].
- [24]A. Bedolla-Jacuinde, S. Aguilar and B. Hernández, "Eutectic Modification in a Low-Chromium White Cast Iron by a Mixture of Titanium, Rare Earths, and Bismuth: I. Effect on Microstructure", *Journal of Materials Engineering and Performance*, vol. 14, no. 2, pp. 149-157, 2005. Available: 10.1361/10599490523300.
- [25]"Hauser & Miller - Casting Tips", *Hauserandmiller.com*, 2019. [Online]. Available: <http://www.hauserandmiller.com/reference/casting.html>. [Accessed: 28- May- 2019].
- [26]"Abrasive Wear - an overview | ScienceDirect Topics", *Sciencedirect.com*, 2019. [Online]. Available: <https://www.sciencedirect.com/topics/materials-science/abrasive-wear>. [Accessed: 28- May- 2019].
- [27]K. Zum Ghar, *Microstructure and Wear of Materials*, 1st ed. 1987.
- [28]M. Atabaki, S. Jaffari and H. Abdollah-pour, "Abrasive Wear Behavior of High Chromium Cast Iron and Hadfield Steel-A Comparison", *JOURNAL OF IRON AND STEEL RESEARCH, INTERNATIONAL*, 2012. [Accessed 28 May 2019].

## 9.0 Appendices

### Appendix A – Titanium Addition Microstructure Images



**Figure 44: A05 alloy with 0.5 wt. % Ti**

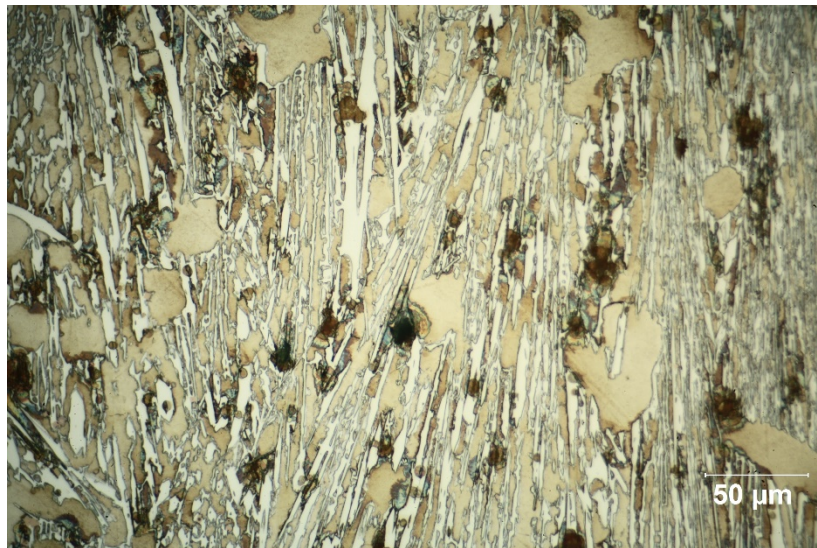


**Figure 45: A05 alloy with 1.0 wt. % Ti**





**Figure 46: A05 alloy with 2.0 wt. % Ti**

### ***Appendix B - Niobium Addition Microstructure Images***

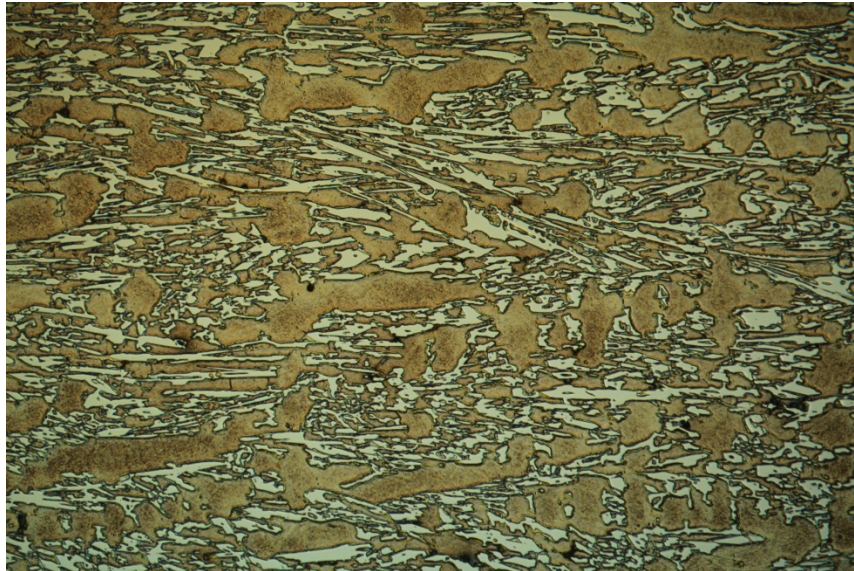


**Figure 47: A05 alloy with 0.5 wt. % Nb**



**Figure 48: A05 alloy with 1.0 wt. % Nb**

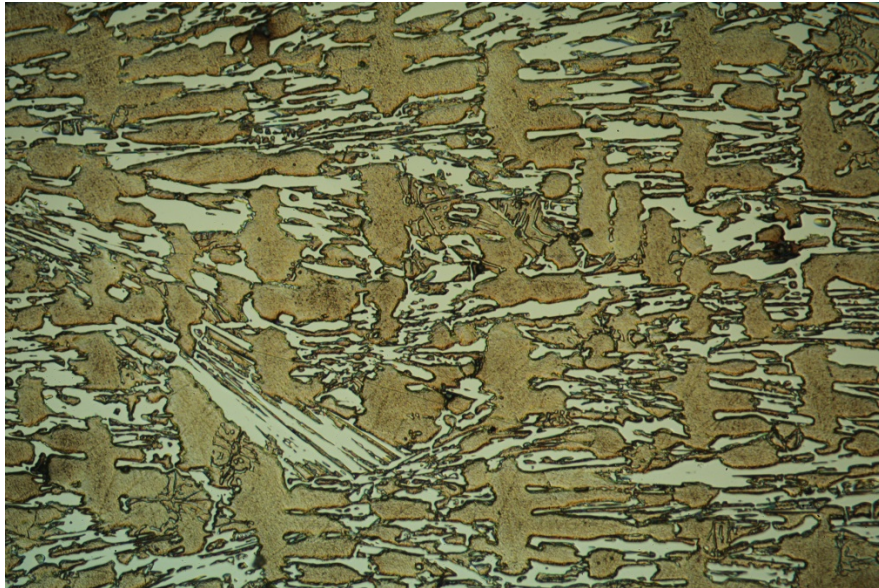


**Figure 49: A05 alloy with 2.0 wt. % Nb**

**Appendix C – Destabilization Treatment Images**

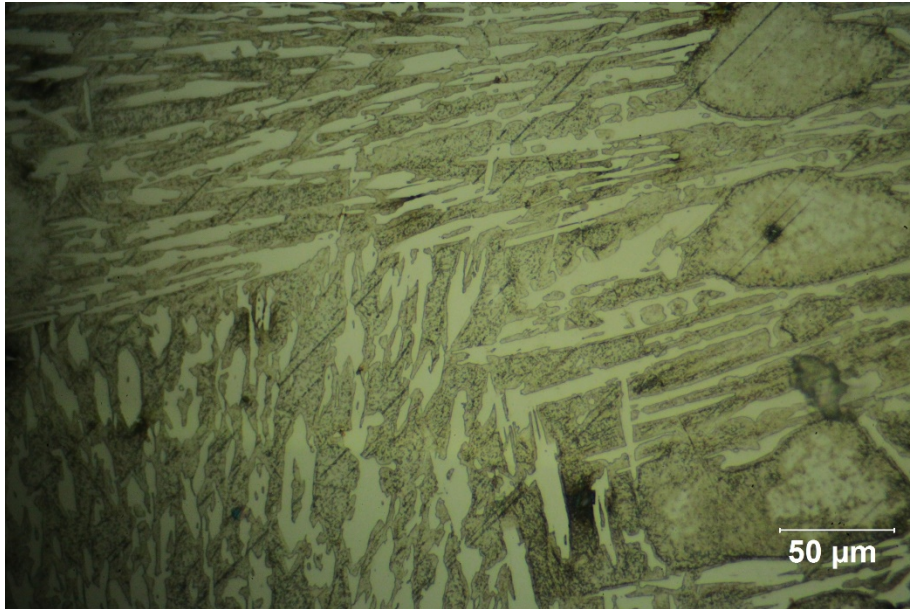


**Figure 50: A05 alloy heat treated at 950<sup>0</sup>C for 6h**

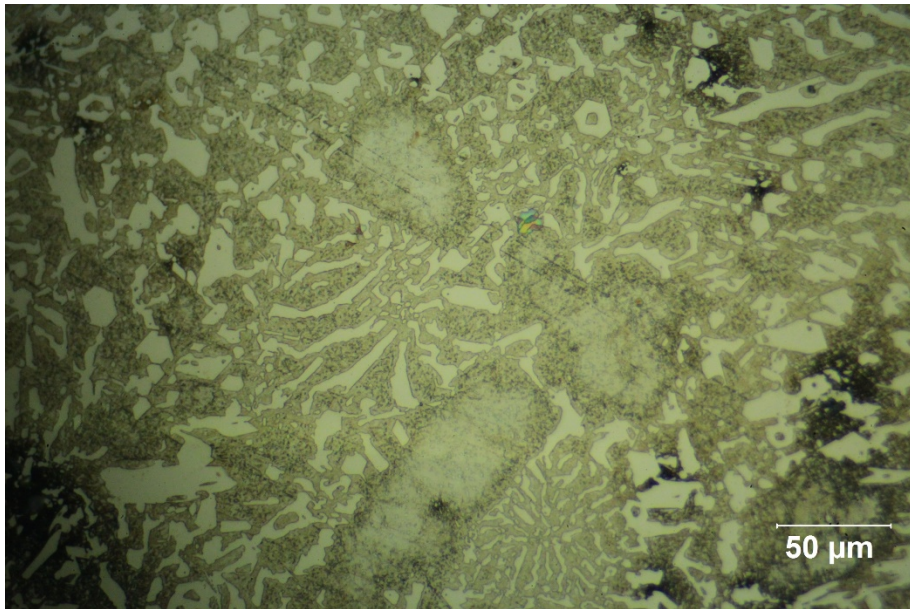


**Figure 51: A05 alloy heat treated at 1020<sup>0</sup>C for 6h**

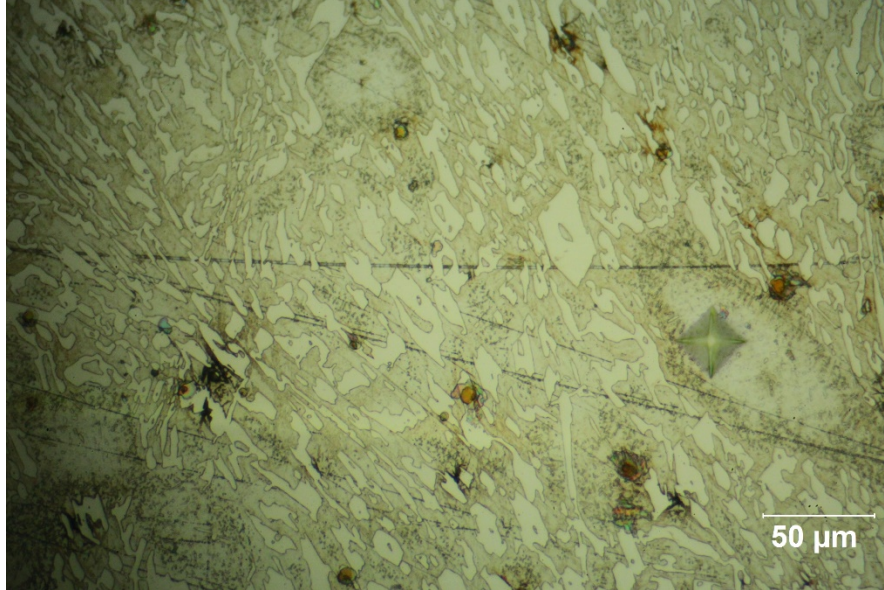


**Figure 52: A05 alloy heat treated at 1080°C for 6h**

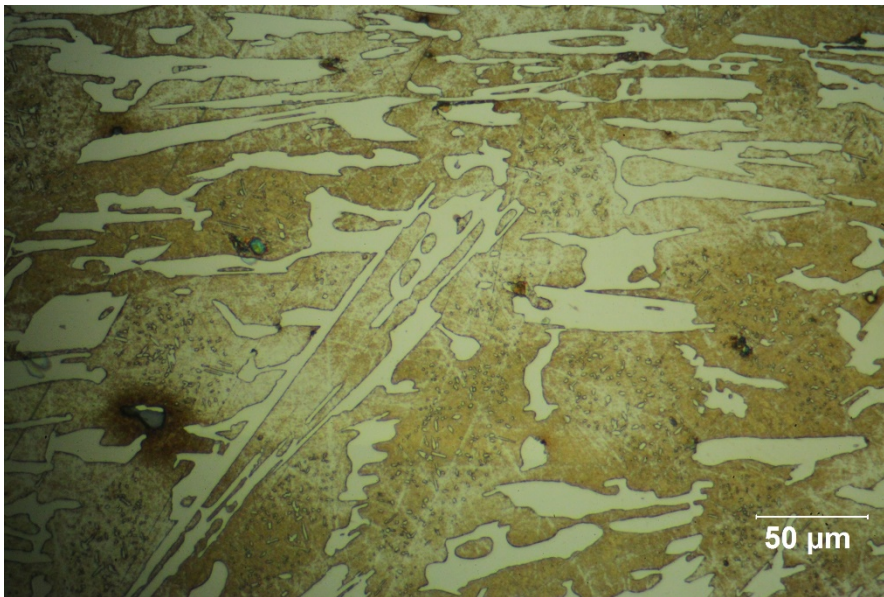


**Figure 53: A05 alloy heat treated at 1190°C for 6h**

**Appendix D – Tempering Treatment Images**

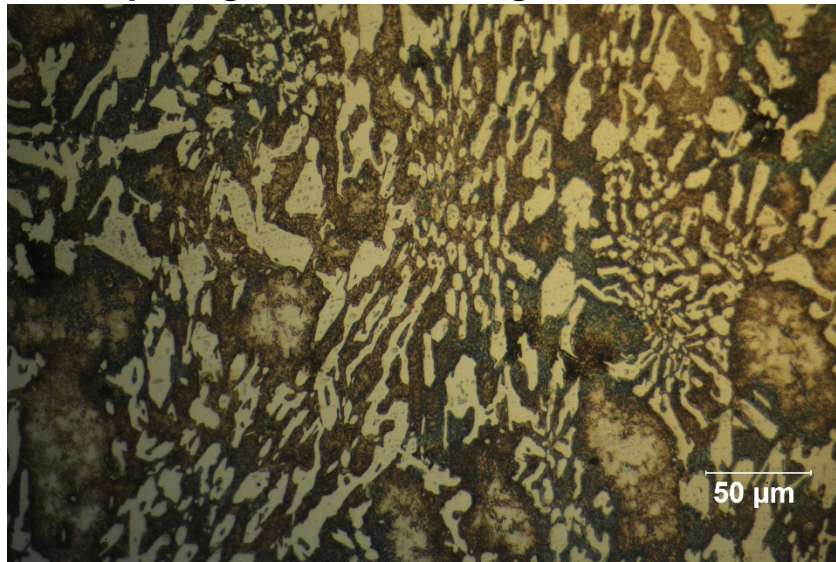


**Figure 54: A05 alloy tempered at 260<sup>0</sup>C for 3h**

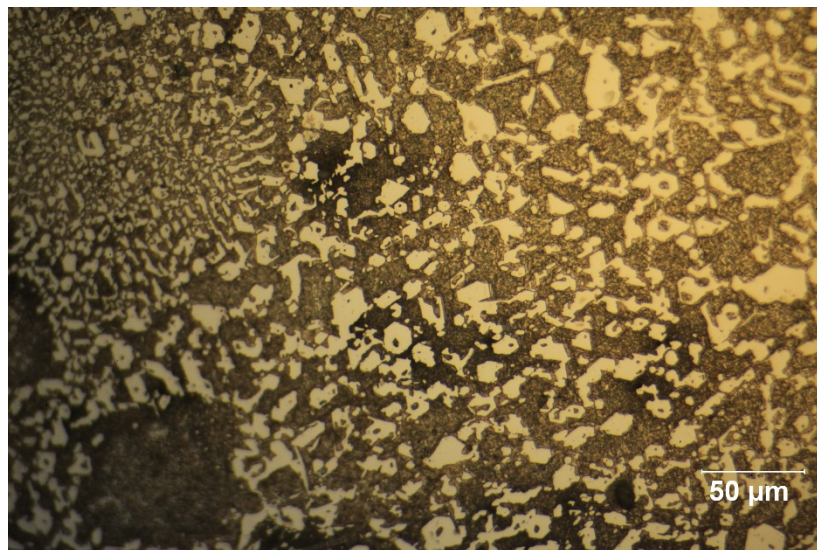


**Figure 55: A05 alloy tempered at 320<sup>0</sup>C for 3h**

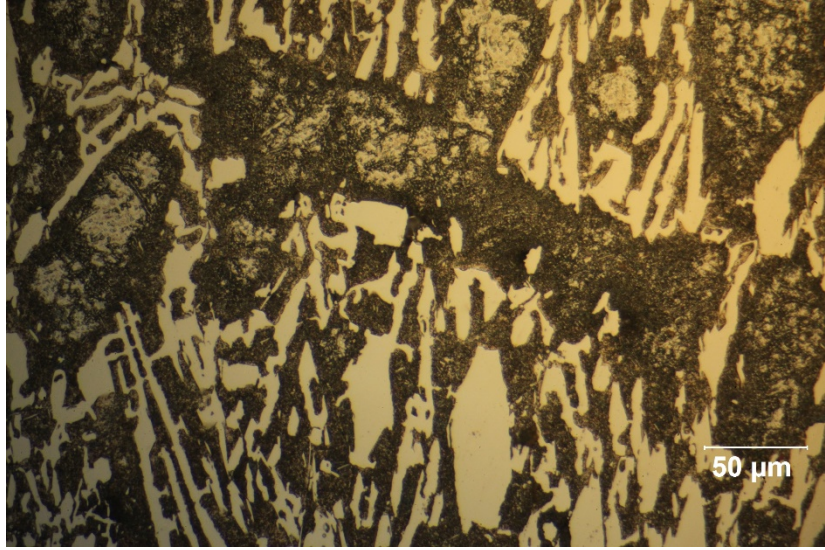


**Figure 56: A05 alloy tempered at 600°C for 3h**

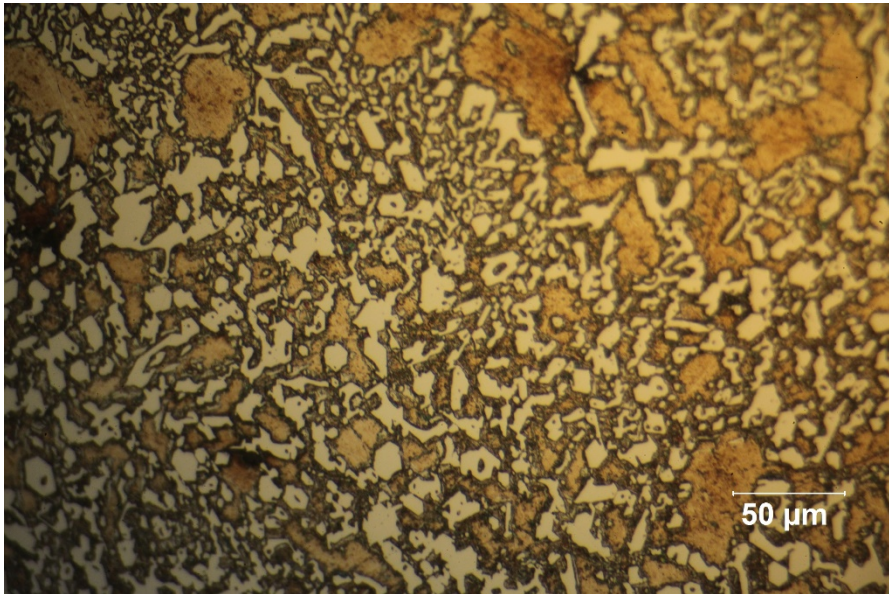


**Figure 57: A05 alloy in the as-cast state**

## Appendix E – Experimental Equipment Images



Figure 58: Furnace used for destabilization treatment & tempering



Figure 59: Polyfast resin used for sample mounting



**Figure 60: Coke used to prevent oxidation during heat treatment**